DESIGN AND ANALYSIS OF HYBRID HORIZONTAL TURBINE

A Final Year Project Report

Presented to

SCHOOL OF MECHANICAL & MANUFACTURING ENGINEERING

Department of Mechanical Engineering

NUST

ISLAMABAD, PAKISTAN

In Partial Fulfillment

of the Requirements for the Degree of

Bachelors of Mechanical Engineering

by

Hammad Khan

Muhammad Zun Nooren Bangash

Muhammad Saad Raza

Hafsa Sajjad

June 2021

EXAMINATION COMMITTEE

We hereby recommend that the final year project report prepared under our supervision by:

HAMMAD KHAN	00000211857
MUHAMMAD ZUN NOOREN BANGASH	00000209195
MUHAMMAD SAAD RAZA	00000211032
HAFSA SAJJAD	00000222366

Titled: “DESIGN AND ANALYSIS OF HYBRID HORIZONTAL TURBINE” be accepted in partial fulfillment of the requirements for the award of BACHELORS IN MECHANICAL ENGINEERING degree with grade _______

Supervisor:	Dr. Emad Ud Din, H.O.D. Mechanical, SMME	Dated:
Committee Member:	Dr. Muhammad Safdar, Assistant Professor, SMME	Dated:
Committee Member:	Dr. Mian Ashfaq Ali, Assistant Professor, SMME	Dated:

______________________ ___________________

(Head of Department) (Date)

COUNTERSIGNED

Dated: ________________ _________________________

(Dean / Principal)

ABSTRACT

This thesis is intended to describe the theoretical solution to our final year project, Design and Analysis of a Horizontal Hybrid Turbine. The project was aimed at giving the proof of concept for a hybrid turbine, i.e., a turbine that is capable of operating in both air and water, so that it can be used to harness power from both media (air and water) throughout the year without any interruption. The power goal was set to 500-1000 watt, enough to power a typical household.

The main issue we faced during our project was the lack of availability of previously existing literature and design content. We had to combine calculations and design concepts of air and water turbine to get the required variables.

Our main concern was the blade design. Turbine model is created using **SolidWorks**. Turbine blade parameters calculations are performed using **MATLAB** and **QBlade**. For analysis of structural integrity and power production capacity, **ANSYS** was used. During the design phase, the portability of the turbine was kept in mind.

However, the generator selection, transmission system design and reconfiguration mechanism were also a part of our project. Some work was done on the hydrokinetic turbine by a group last year which was capable of producing 80-90 watts. Our goal was not only to scale up the power capacity of the turbine but also to make it work in air as well.

Our target was to design and optimize the turbine for the northern areas of the Pakistan where there are lots of rivers and streams which could be utilized to produce power. Also, to ensure the uninterrupted power supply in winters when water if usually frozen or limited, we had to make the turbine operable in air as well.

We had to ensure significant power generation for both air and water, while keeping the blade length minimum to ensure portability. We achieved quite reasonable results: two-fold of targeted power production in case of water and around 90% of the targeted power production in case of air medium, while keeping size and strength constraints in check.

ACKNOWLEDGEMENTS

First and foremost, we thank **ALLAH Almighty** for HIS blessings which allowed us to complete the project efficiently and effectively.

Then we would like to extend our gratitude to our supervisor ***Dr. Emad-ud-Din*** and co-supervisor ***Dr. Aamir Mubashir*** for helping us in every phase of the project. We would also like to thank our colleague ***Wasif Rehman*** for specifically helping us with the calculation part of the project on MATLAB. Furthermore, we thank ***Sir Asfandyar*** for helping and guiding us throughout the project. The techniques and knowledge he imparted to us regarding the analysis of the project on ANSYS was very valuable. The analysis part of the project would not have been possible without his assistance and guidance.

Finally, we thank ***our parents*** for continuous prayers and moral support. What we achieved was only possible because of them.

ORIGINALITY REPORT

plagcheck1

ORIGINALITY REPORT

7%	5%	2%	4%
SIMILARITY INDEX	INTERNET SOURCES	PUBLICATIONS	STUDENT PAPERS

PRIMARY SOURCES

1	www.gracedesideriorealtor.com Internet Source	1%
2	www.intechopen.com Internet Source	1%
3	docplayer.net Internet Source	<1%
4	Submitted to Frederick University Student Paper	<1%
5	Submitted to University of Portsmouth Student Paper	<1%
6	Submitted to University of Hull Student Paper	<1%
7	ich.unesco.org Internet Source	<1%
8	www.scielo.org.mx Internet Source	<1%
9	Submitted to University of Nottingham Student Paper	<1%

Table of Contents

List of Tables

List of Figures

ABBREVIATIONS

TSR	Tip Speed Ratio
AoA	Angle of Attack
HAWT	Horizontal Axis Wind Turbine
VAWT	Vertical Axis Wind Turbine
CFD	Computational Fluid Dynamics
SDGs	Sustainable Development Goals

NOMENCLATURE

P_w	Power for water configuration (W)
P_a	Power for air configuration (W)
ρ_w	Density of water (kg/m^3)
ρ_a	Density of air (kg/m^3)
μ_w	Dynamic viscosity of water $(kg/m.s)$
μ_a	Dynamic viscosity of air $(kg/m.s)$
V_w	Velocity of water (m/s)
V_a	Velocity of air (m/s)
$C_{p,w}$	Power coefficient for water configuration
$C_{p,a}$	Power coefficient for air configuration
λ_w	TSR for water configuration
λ_a	TSR for air configuration
η_o	Overall efficiency
n	Number of blades
Θ	Pitch angle of turbine for water configuration
β	Angle of twist of turbine
r_w	Blade radius/length for water configuration (m)
r_a	Blade radius/length for air configuration (m)
r_{avg}	Combined/average blade radius/length (m)
r_{inc}	Increment in blade radius/length for relative value (m)
λ_i	Modified TSR for water configuration
k	Number of blade profile sections
ω_w	Rotational speed for water configuration (rad/s)
ω_a	Rotational speed for air configuration (rad/s)
N_w	RPM for water configuration
N_a	RPM for air configuration
a	Axial induction factor for water configuration
a'	Tangential induction factor for air configuration
Φ	Relative flow angle for water configuration

Ma_w	Mach number for water configuration
Ma_a	Mach number for air configuration
Re_w	Reynold's number for water configuration
Re_a	Reynold's number for air configuration
Re_{avg}	Combined/average Reynold's number
α_w	Angle of attack for water configuration (°)
α_a	Angle of attack for air configuration (°)
α_{opt}	Combined optimum angle of attack (°)
c_w	Chord length at tip for water configuration (m)
c_a	Chord length at tip for air configuration (m)
c_{avg}	Combined/average chord length at the tip (m)
c_{sec}	Chord length at a section (m)
ac_{sec}	Aerodynamic Centre of a chord section (m)
$C_{L,w}$	Coefficient of lift for water configuration
$C_{L,a}$	Coefficient of lift for air configuration
$C_{D,w}$	Coefficient of drag for water configuration
$C_{D,a}$	Coefficient of drag for air configuration
$(\frac{C_L}{C_D})_{max,w}$	Maximum value of lift-to-drag ratio for water configuration
$(\frac{C_L}{C_D})_{max,a}$	Maximum value of lift-to-drag ratio for air configuration
C_m	Coefficient of Moment

1 INTRODUCTION

Northern areas of Pakistan are blessed with lots of rivers and streams which are a potential power source if utilized properly. Unfortunately, there are not many active projects to harness this energy from these sources. A few locally made turbines known locally as “Junder” (جندر) are operating in many areas but they produce very limited power. The best solution to utilizing these sources are hydrokinetic turbines which utilize kinetic energy of the moving water to produce power. Some work has been done on hydrokinetic turbines in the past years. However, their usage in northern areas was limited to summers only as there is enough water flow available in rivers and streams during summers. In winters, however, the water either freezes or its flow is limited which makes the use of hydrokinetic turbines not so practical during those days. In short, a household totally relying on its own power production from the water sources available in the area will have to find a way to ensure the power supply during the days of inactivity of hydrokinetic turbines.

Keeping in mind the economics of the case, the only solution that seems feasible is to enable the turbines to work in both wind and water so that the power supply becomes independent of the weather conditions and availability of water. Although there are many complications related to the geography of the area where the turbine will be working and the turbine design itself as water turbines require strong blades to withstand the water pressures and the wind turbines need to be light in weight to perform well.

What we have to do is to design a horizontal-axis hybrid turbine that can not only produce power in both wind and water but also is easy is install during media switching (i.e., air and water). The power output of the turbine is supposed to reach around 500-1000 watt so that it can power a typical household. The configuration mechanism of turbine should be designed too for this purpose. Our main purpose is to provide the proof of concept as no work has been done in this regard. The feasibility of the turbine, however, is not in the scope of our project.

1.1 Motivation of Work

Following is the motivation behind the project:

1.1.1 Detrimental Impact of Unclean Energy

The non-renewable energy such as fossil fuels will ultimately run out so the world is looking for feasible alternatives such as hydro and solar energy. The non-renewable traditional energy sources such as fossil fuels are pumping loads of CO2 into the atmosphere causing greenhouse effect and the rise of temperatures globally. The rise in global temperature and the melting of icebergs in polar region is causing rise of sea levels which will lead to the drowning of coastal areas. Pakistan is also in the top 10 most vulnerable countries to climate change. 80% of our water comes from glaciers which are continuously depleting due to greenhouse impact and rise of global temperatures

1.1.2 High Demand for Cheaper Energy

The energy obtained from non-renewable sources such as coal and oil are very expensive for industry and non-commercial users. There is a need to shift to renewable energy sources to meet the growing demands for cheaper energy. Cheaper energy allows the industry to produce goods at lower price so it's easier to compete with other countries. Cheaper energy also makes it affordable for a common man to manage his monthly expenses. In Pakistan, we produce electricity at an expensive rate compared the other regional countries such as India and Bangladesh, this makes it difficult for Pakistani Industry to capture global industrial orders, so there is a need to shift to cheaper renewable energy.

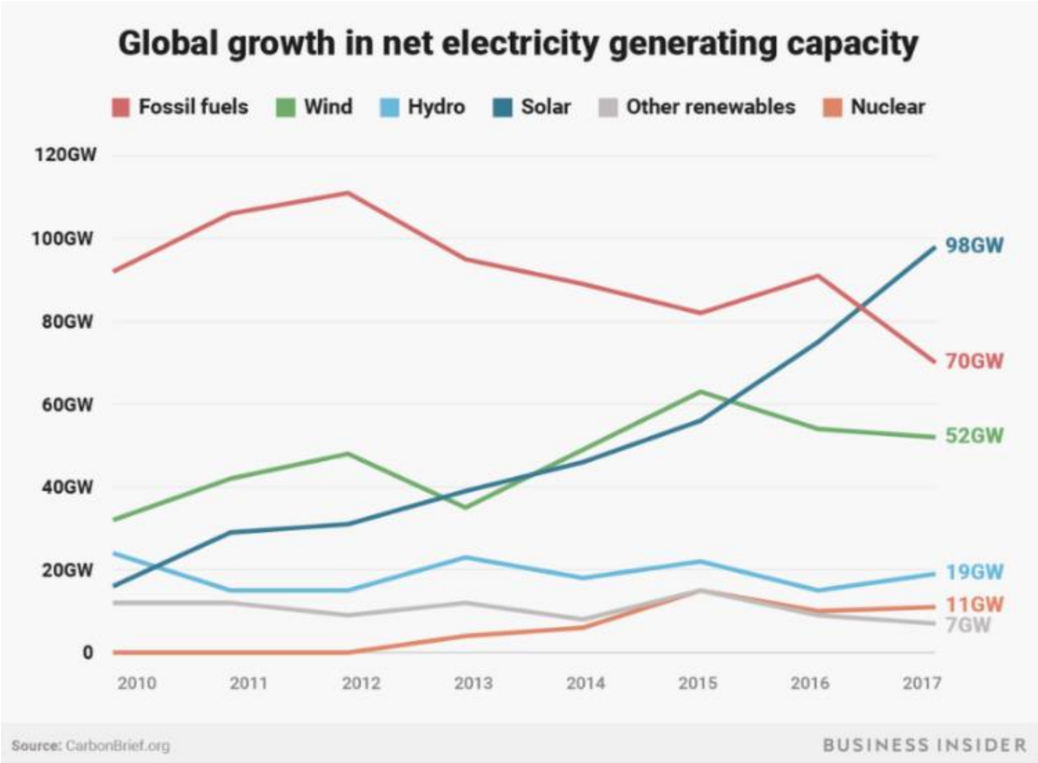

Figure 01: Growing Demand for Cheaper Renewable Energy

1.1.3 Energy Access for Remote Areas

Supplying energy to remote areas can be a difficult task. Taking transmission lines to remote areas is very difficult because of land losses and expensive management. Using non r4enewable energy here will prove harmful for the environment. So, the best solution here is to utilize the natural resources such as wind and water energy to produce and provide energy to remote areas locally. This will decentralize the energy grid and distribution system, create cheap energy affordable to local people and this will have no harmful impact on the environment.

1.1.4 Sustainable Development Goals

The project meets the sustainable development goals. The project accounts for changing climatic situation, taking in to account rising global temperatures and pollution and therefore providing a sustainable, long-term economic solution.
Following SDGs are targeted through our project:

1. SDG 07: Affordable and Clean Energy
2. SDG 09: Industry, Innovation and Infrastructure
3. SDG 11: Sustainable Cities and Communities
4. SDG 12: Responsible Consumption and Production
5. SDG 13: Climate Action

Figure 02: SDGs covered by Horizontal Hybrid Turbine Project

1.2 Problem Statement

As the fossil fuel reserves deplete, the world is fast moving towards renewable technologies. Among renewable energies, hydro and wing energies are most reliable and cheap source of renewable energy. Large dams are a good source of renewable energy but they take a lot of time and resource to construct. The Dams cannot be constructed at any place, they can only be built in specific places based on dam site evaluation.

To provide electricity in remote areas, hydrokinetic turbines are a good option, they are cheaper and easy to install. However, the problem with hydrokinetic turbines is that during winter the flow in rivers and streams decreases causing the power production of hydrokinetic turbine to fall significantly. Wind turbine can be used in these regions as well but the issue with wind turbine is that wind turbines have lower power production compared to hydrokinetic turbines for the same blade radius.

Our proposed solution is to use a hybrid turbine that can act as a hydrokinetic turbine in the summer and wind turbine in winter season. Since the water discharge is high in summers, power production will be high when using water medium and in winters when river flow discharge will be low, the hybrid turbine can be used as a wind turbine to ensure power supply throughout the year.

1.3 Objectives

The project's primary objective is to develop a Horizontal Hybrid Turbine which can be used in water and wind medium. The turbine will be able to work in remote areas like northern areas of Pakistan and whole system including turbine transmission gear and generator will give a net power output of 500-1000 watts. This will be enough to power a single household.

Following are the objectives:

1- Design and analysis of portable hydrokinetic turbine which can operate in both air and water
2- Implementation of optimized blade design for use in air and water

3- Scaling up the power production capacity of the turbine to enable it to power a single household
4- Analysis of the power coefficient and structural integrity using numerical simulations

2 LITERATURE REVIEW

From the literature review, no significant material was found specifically referring to our project. Some work has been done on the hydrokinetic turbines and even on the portable hydrokinetic turbines, however, the hybrid turbines field has not yet been explored so far.

2.1 Turbine

A turbine is a device that harnesses the kinetic energy of some fluid - such as water, steam, air, or combustion gases - and turns this into the rotational motion of the device itself.

2.1.1 Working principle

Turbines work on a simple principle, they have 2, 3 or more propeller type blades which are turned around the rotor by the force of the working fluid acting on them. This turning rotor via a shaft is used for the production of power through a generator. Basic schematic of a turbine is shown below:

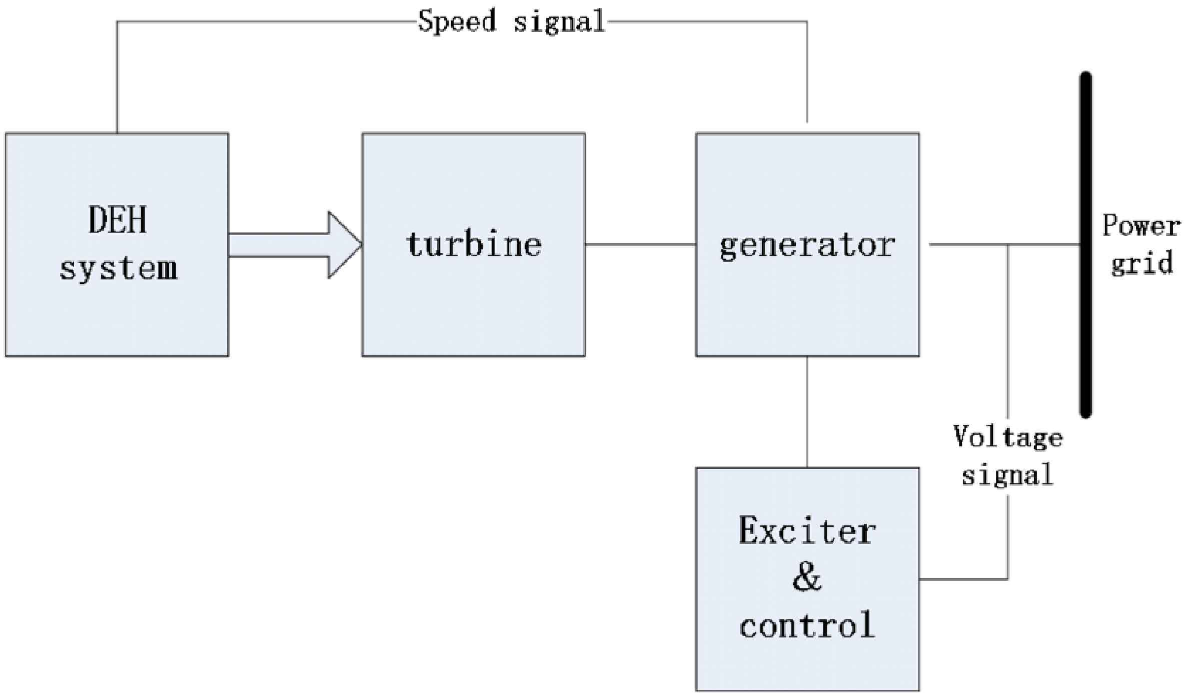

Figure 03: Turbine Working Principle

2.2 Turbine Types

A general overview of a few types of turbines is given below:

2.2.1 On the Basis of Orientation

On the basis of orientation, turbines are divided into two main types:

2.2.1.1 Horizontal Axis Turbine: Their axis of rotation is parallel to the general direction of fluid flow

2.2.1.2 Vertical Axis Turbine: Their axis of rotation is perpendicular to the general direction of fluid flow

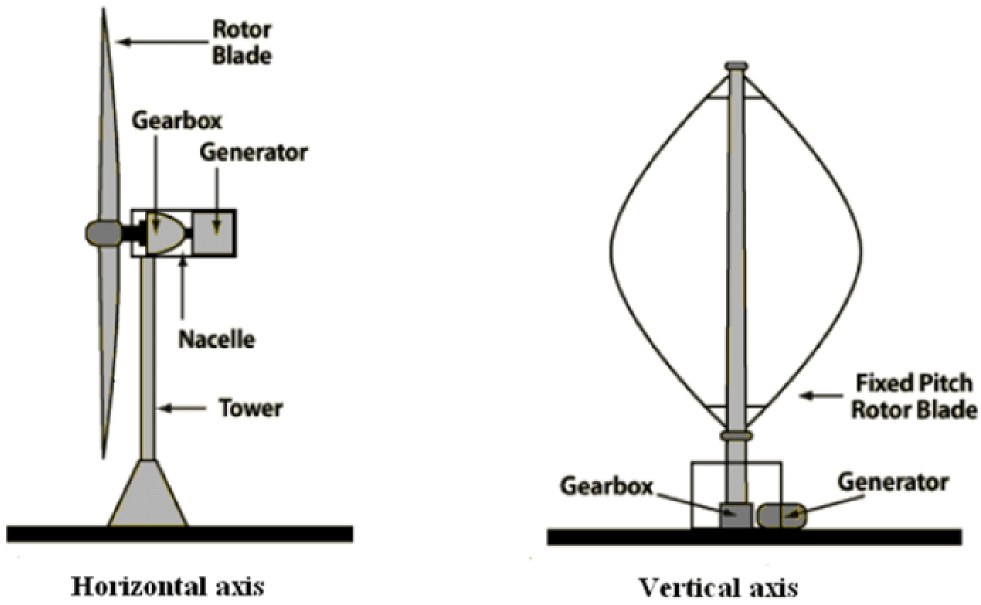

Figure 04: Horizontal Axis versus Vertical Axis Turbines

2.2.2 Main Differences between Horizontal & Vertical Axis Turbines

Although Vertical Axis Turbines have the advantage of accepting fluid flow from any direction, still, *a horizontal turbine is preferred* because of the following characteristics:

1. More power production capacity
2. Low infrastructure
3. More efficiency
4. Less environmental impacts
5. Less noise
6. Less space requirement
7. Easy installation
8. Easy maintenance

2.2.3 On the Basis of Working Fluids

There are many types of turbines on basis of working fluid but the most commonly used are:

2.2.3.1 Wind Turbines

The wind turbines, as name suggests, uses the *kinetic energy of wind* to produce power. The wind itself is caused by the combination of following concurrent events:

i. The sun unevenly heating the atmosphere
ii. Irregularities of the earth's surface
iii. The rotation of the earth

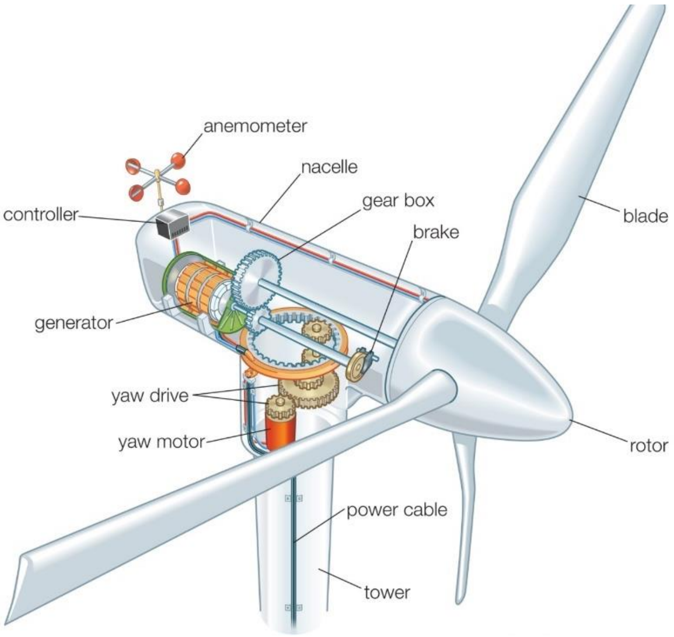

Figure 05: Wind Turbines

Wind Turbines are classified on the basis of their orientation as:

2.2.3.1.1 **Horizontal Axis Wind Turbine:** Also known as HAWT, rotates parallel to the wind flow.

2.2.3.1.2 **Vertical Axis Wind Turbine:** Also known as VAWT, rotates perpendicular to the wind flow.

2.2.3.2 Water Turbines

Water Turbines utilize energy from water to produce the power.

There are two main types of Water Turbines:

2.2.3.2.1 **Hydrostatic Turbines:** They use the potential energy of the stored water falling from a height to produce power

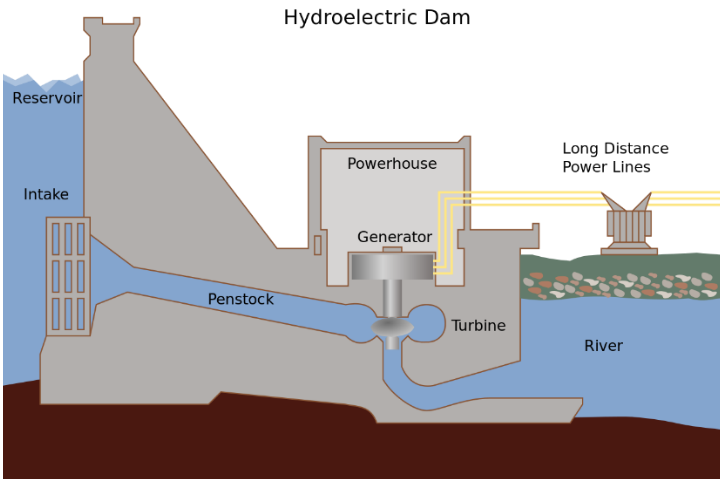

Figure 06: Hydrostatic Turbines

2.2.3.2.2 Hydrokinetic Turbines: They use the kinetic energy of the flowing water to produce energy (Similar to Wind Turbines).

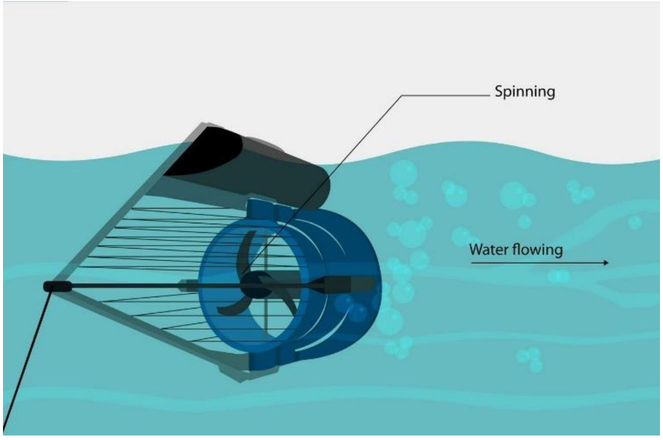

Figure 07: Hydrokinetic Turbines

2.2.4 Main Differences between Wind & Water Turbines

1. ***Power Production Capacity:*** With size and other parameters constant, Water turbine is capable of producing more power than wind turbine. This is because the density of water is higher than air.
2. ***Size:*** Wind Turbines tend to be much larges in size than the water turbines
3. ***Material Properties:*** They are of prime importance when it comes to various turbines. Water turbine blades are supposed to be stronger as they have to withstand high pressures exerted by water.

2.3 Design Parameters

2.3.1 Power Coefficient

Power Coefficient is defined as the limit up to which a turbine can extract power from the fluid causing it to operate. The reason for this is that for the turbine to completely extract all the power from the fluid it should come to rest after passing through the turbine. The maximum value of the extracted power is defined as Betz limit and its value is 0.593.

Total power available in the working fluid is given as:

$$P_{total} = \frac{1}{2}\rho A v^3$$

Where, ρ is fluid density, A is swept area and v is fluid freestream velocity

Power extracted or produced by the turbine is given as:

$$P_{turbine} = T\omega$$

Where, T is torque and ω is rotational velocity

The power coefficient can be calculated by the following equation:

$$C_p = \frac{P_{turbine}}{P_{total}} = \frac{T\omega}{\frac{1}{2}\rho A v^3}$$

This leads to another way of defining C_p, the ratio of mechanical power of rotor to the power available in the fluid.

2.3.2 Tip Speed Ratio

It is a very important design parameter for turbines. TSR is defined as the ratio of tangential velocity of the fluid at the tip of the blade to the fluid freestream velocity.

$$\lambda = \frac{r\omega}{v}$$

Where, λ is TSR, r is blade length, ω is rotational velocity and v is fluid freestream velocity.

An optimum value of TSR is chosen in order to achieve a high value of C_p. All the optimum values of geometric parameters of the rotor are based on TSR. It has been found that efficiency is directly proportional to TSR, however, the value of TSR can be increased to certain limit because aerodynamic and centrifugal stresses, and noise also increase with TSR. The chord width reduces with increasing value of TSR meaning a narrow blade profile so more chances of failure. Hence, the requirement of enhanced structural integrity increases with TSR.

2.3.3 Swept Area

The area in which the flowing fluid makes contact with the turbines blade is called swept area. In other words, the area swept by the blades of the turbine as observed from front. It is a very essential parameter in turbine design. It determines the size of the turbine. The portability is greatly affected by swept area.

$$A = \pi r^2$$

Where, A is swept area and r is blade radius. This is defined for horizontal axis turbine. For vertical axis is given as,

$$A = D \times H$$

Where, 'D' is the diameter and 'H' is height.

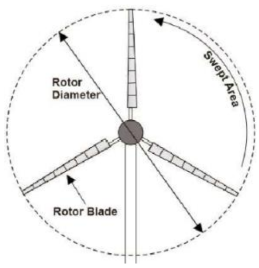

Figure 08: Swept Area for Horizontal Axis Turbine

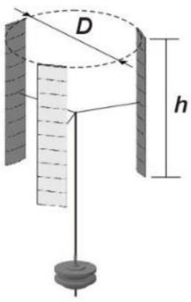

Figure 09: Swept Area for Vertical Axis Turbine

The swept area directly effects the power production of the turbine; however, it also leads to increase in cost and material requirements. Hence, the swept area should be chosen as to balance power production, cost and material requirements.

2.3.4 Angle of Attack

The angle between in the incoming fluid flow to the chord line is termed as angle of attack. Angle of attack affects the operation of turbine and its power production. Its value also changes the value of stresses that are produced on the blades of the turbine. In literature it is usually expressed as α. The angle of attack value is selected as to maximum lift-to-drag ratio.

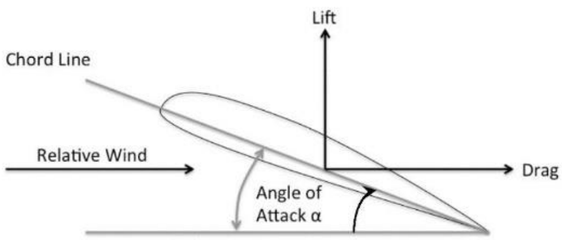

Figure 10: Angle of Attack

2.3.5 Angle of Twist

Angle between chord line and rotor plane is termed as angle of twist, represented as β. It is dependent upon desired angle of attack and TSR. It can also be defined as the difference between angle of attack and relative flow angle. It leads to increase power production but also to complexities in manufacturing. So, sometimes the angle of twist is reduced to simplify manufacturing and cut cost but comprises power production, an optimum value is to be selected. Twist angle shows torsion of the blade. It is termed as pitch angle as well.

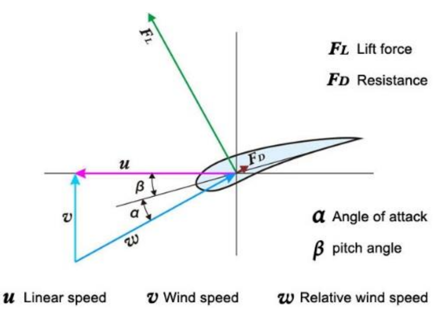

Figure 11: Angle of Twist or Pitch Angle

2.4 Hybrid Turbines

A hybrid turbine, by definition, is a turbine that can operate in both the working fluid, i.e., Air and Water. In past, no work has been done on the hybrid turbines. The material that we explored was available separately for the wind turbines and the water (hydrokinetic) turbines. So far, no one has explored the common area to find a solution to the hybrid turbines.

3 METHODOLOGY

As discussed in the literature review, no work has been done previously on the hybrid turbines. So, for the rotor design, we used the data available for the wind and hydrokinetic turbines to calculate the initial parameters analytically and after finding the suitable middle grounds for the parameters, we made an initial design. Then this design was tested and tweaked analytically to get verification for our initial assumptions and design. Also, the generator selection and the transmission system design were done according to our requirements and the available data. Lastly, the Reconfiguration Mechanism was decided & designed.

3.1 Initial Data

The properties for both the media (air & water) were available to us. Wind turbines are not feasible under 5 m/s wind speed. Also, generally, the wind turbines are designed at 7 m/s wind speeds. Similarly, initial data for the water turbine was also available. The overall efficiency of the turbine was taken as 70%. Also, the value of power coefficient for wind turbine was assumed to be 0.45 from the historical data. The following table summarizes the initial parameters used for our design and analysis:

Sr. No.	Parameter	Value	Unit
1.	Wind Velocity	7	m/s
2.	Water Velocity	1.6	m/s
3.	TSR Wind	7	$-$
4.	TSR Water	5	$-$
5.	Wind Density	1.0585	kg/m^3
6.	Water Density	998	kg/m^3
7.	Dynamic Viscosity (Wind)	0.00002857	kg/m^2s^2
8.	Dynamic Viscosity (Water)	0.001002	kg/m^2s^2
9.	Required Power	1000	W
10.	Efficiency	70	%
11.	Power Coefficient for Wind Turbine	0.45	$-$

Table 01: Initial Parameters

3.2 Rotor Design

All the steps and methodology used for rotor design is discussed in detail below:

3.2.1 Pre-Design Calculations

3.2.1.1 Blade Length Calculations

For starters, we needed to know the length of the turbine blades for the simplest scenario. For that purpose, firstly, the values for power coefficients (C_p) for both wind and water turbines were needed. The value of C_p for wind turbine was assumed to be 0.45 as their values generally fall in the range of 4-6. For the power coefficient of Water component, we used the analytical relations found from the literature for different attack angles to iterate and converge to a suitable value of Cp.

The interrelated formulas used for iterations are:

$$\frac{1}{\lambda_i} = \frac{1}{\lambda + 0.008\theta} - \frac{0.035}{\theta^3 + 1}$$

$$C_p(\lambda, \theta) = 0.22\left(\frac{116}{\lambda_i} - 0.4\theta - 5\right)e^{\frac{-12.5}{\lambda_i}}$$

With value of required power already known, i.e., 1000 watt, using the value of Cp and with the incorporation of overall efficiency in the formula shown below, we calculated the values of radius for the both wind and water components. The formula used is shown below:

$$P = \frac{1}{2}\rho \times \pi r^2 \times v^3 \times C_p \times \eta_0$$

After calculating blade lengths separately for the wind and water cases, their average was taken in order to get the blade length for the Hybrid Turbine case.

3.2.1.2 Chord Lengths at Sections Calculations

We had divided the entire Blade into 10 parts. The Value of the chord length was calculated at the tip of thew blade and then was translated towards the base of the blade using a linearized model. The reason for using a linearized model was the design and manufacturing simplicity.

The Chord Length at a section is related to lift and drag coefficients of the airfoil. The lift and drag coefficients are obtained from a plot of the airfoil against a specific Reynold’s number. The Reynold’s number itself is obtained from the Chord’s length. So, in order to obtain the Chord Length, software XFoil was integrated with MATLAB to iterate and read the values of Lift and Drag Coefficient for the selected airfoil geometry against various Reynold’s Number values and Solve for the Chord Length value at a maximum Lift-to-Drag condition.

3.2.1.2.1 Steps Involved

The methodology and formulae used for the chord length calculations in case of water configuration are shown below.

For the calculation of axial induction factor:

$$C_p = \frac{4a(1-a)^2}{\eta}$$

The tangential induction factor was calculated from axial induction factor using the formula:

$$\acute{a}(1+\acute{a})\lambda^2 = a(1-a)$$

Then the relative angle was calculated using the formula:

$$tan\phi = \frac{1-a}{\lambda(1+\acute{a})}$$

Lastly, the chord length for water was calculated as:

$$c = \frac{8\acute{a} \times r \times \lambda \times sin^2\phi}{(C_L sin\phi - C_D cos\phi) \times n_{blade} \times (1-a)}$$

In the case of wind, the chord length was calculated from the formula:

$$c = \frac{16\pi r}{9nC_L\lambda\sqrt{\lambda^2 + \frac{4}{9}}}$$

Where the value for C_L was obtained from XFoil-MATLAB Integration as mentioned before.

After the Chord Length was determined, it was translated to other sections through the linear increments. All the calculations mentioned above were done on MATLAB.

3.2.2 Airfoil Selection

3.2.2.1 Series Selection

Mostly, NACA foils are used in the turbine design. There were many options from NACA airfoils series such as NACA 4-digit series, 5-digit series, 4-/5-digit series, 6-series and 8-series. NACA 4-digit series, although used widely in past were not a good choice as there are better options available. Similarly, NACA 6-series and NACA 8-series were also not viable as they are very complex in geometry and thus manufacturing. Therefore, NACA 5-digit series was selected. There were many reasons for this selection such as:

1. Their higher maximum lift coefficient
2. Low Pitching moment
3. They are least affected by roughness

NACA Five-Digit Series:
The NACA Five-Digit Series uses the same thickness forms as the Four-Digit Series but the mean camber line is defined differently and the naming convention is a bit more complex. The first digit, when multiplied by 3/2, yields the design lift coefficient (c_l) in tenths. The next two digits, when divided by 2, give the position of the maximum camber (p) in tenths of chord. The final two digits again indicate the maximum thickness (t) in percentage of chord. For example, the NACA 23012 has a maximum thickness of 12%, a design lift coefficient of 0.3, and a maximum camber located 15% back from the leading edge. The steps needed to calculate the coordinates of such an airfoil are:

1. Pick values of x from 0 to the maximum chord c.
2. Compute the mean camber line coordinates for each x location using the following equations, and since we know p, determine the values of m and k_1 using the table shown below.

$$y_c = \frac{k_1}{6}\left[x^3 - 3mx^2 + m^2(3-m)\,x\right] \qquad \text{from } x = 0 \text{ to } x = p$$

$$y_c = \frac{k_1\, m^3}{6}(1-x) \qquad \text{from } x = p \text{ to } x = c$$

Mean-line designation	Position of max camber (p)	m	k1
210	0.05	0.0580	361.400
220	0.10	0.1260	51.640
230	0.15	0.2025	15.957
240	0.20	0.2900	6.643
250	0.25	0.3910	3.230

3. Calculate the thickness distribution using the same equation as the Four-Digit Series.

Figure 12: NACA Five-Digit Series

3.2.2.2 Selected Airfoil

The airfoil We Selected was NACA 24012 airfoil. This airfoil is widely used in turbines throughout the field. Its geometrical data was generated using a MATLAB Airfoil Generator Code to be used later in the design process. (3)

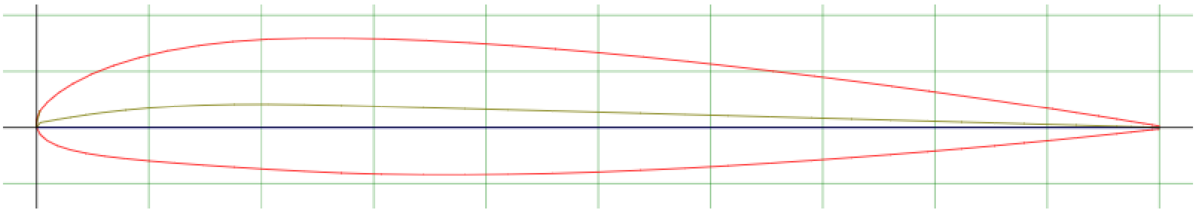

Figure 13: NACA - 24012 Airfoil Geometry

The properties of the airfoil we selected are:

Sr. No.	Property	Value	Unit
1.	Design Lift Coefficient	0.3	$-$
2.	Position of Maximum Camber from Leading Edge	20	$\%\ of\ chord$
3.	Maximum Thickness	12	$\%\ of\ chord$

Table 02: Properties of Selected NACA 24012 Airfoil

3.2.3 Initial Parametric Results

The calculations were done separately for the wind and water cases to determine the blade lengths, chord lengths and other parameters for both cases.

The initial parametric results are shown below:

Sr. No.	Parameter	Wind	Water	Unit
1.	Power Coefficient	0.450000	0.394163	$-$
2.	Blade Length	2.359350	0.751291	m
3.	Chord Length	0.119274	0.026550	m
4.	Lift-to-Drag Ratio	10.85865	19.77854	$-$
5.	Lift Coefficient	0.493200	0.634100	$-$
6.	Drag Coefficient	0.045420	0.032060	$-$
7.	Reynold's Number	30246.33016	43027.54491	$-$
8.	Angle of Attack	3.45	3.9	$degree$

Table 03: Initial Parametric Results

These values were then averaged to get the parameters for the combined configuration.

Similarly, the pressure distribution obtained for the selected airfoil through QBlade is shown below:

Figure 14: Pressure Distribution over NACA 24012 Airfoil - QBlade Results

3.2.4 Combined Configuration Parameters

After getting separate values for wind and water cases, they were averaged to get the parameters for combined rotor configuration as shown:

Parameter	Value	Unit
Blade Length	1.555320	m
Chord Length	0.072912	m

Table 04: Combined Configuration Parameters

3.2.5 Blade Twist Optimization

With the length, profile, no. of sections and Chord length at each section known, the next step was to incorporate the twist at each section for proper harnessing of energy from the working fluids when in operation. In order to optimize the twist at each section, we used the software tool QBlade. The aerodynamic center is typically at 25% of chord length.

The following table shows the sections of the blade with their profile, chord lengths and the optimized twist:

Section	Section Type	Chord Length at Section (m)	Twist (degree)	Length at Section (m)	Aerodynamic Centre (m)
0	Circular	0.060000	40.98	0.000000	-
1	Circular	0.060000	25.45	0.155532	-
2	Circular	0.080000	17.59	0.311064	-
3	NACA 24012	0.243041	9.71	0.466596	0.060760
4	NACA 24012	0.182281	6.75	0.622128	0.045570
5	NACA 24012	0.145824	4.68	0.777660	0.036456
6	NACA 24012	0.121520	3.17	0.933192	0.030380
7	NACA 24012	0.104160	2.01	1.088724	0.026040
8	NACA 24012	0.091140	1.09	1.244256	0.022785
9	NACA 24012	0.081014	0.35	1.399788	0.020253
10	NACA 24012	0.072912	-0.26	1.555320	0.018228

Table 05: Blade Section Parameters

Also, the value of optimized angle of attack against maximum lift to drag extracted from QBlade data is shown as:

Quantity	Value	Unit
Maximum CL/CD	15.858	–
Angle of Attack	3.3	$degree$

Table 06: Blade Parameters from QBlade

3.2.6 Final Blade Modelling and Rotor Assembly

After getting the final values of all the parameters required for modelling, SolidWorks was used to design the blade and then it was assembled with the hub to create the final Rotor.

The figures below show our designed blade and the rotor assembly:

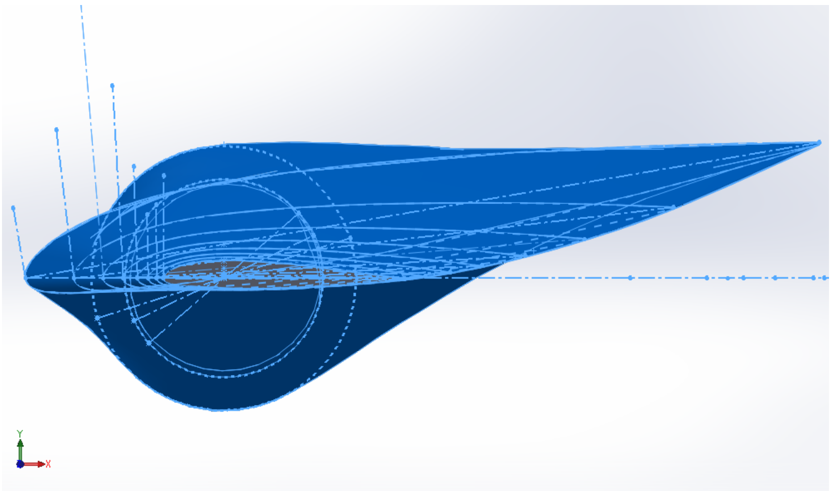

Figure 15: Designed Blade Cross Sections

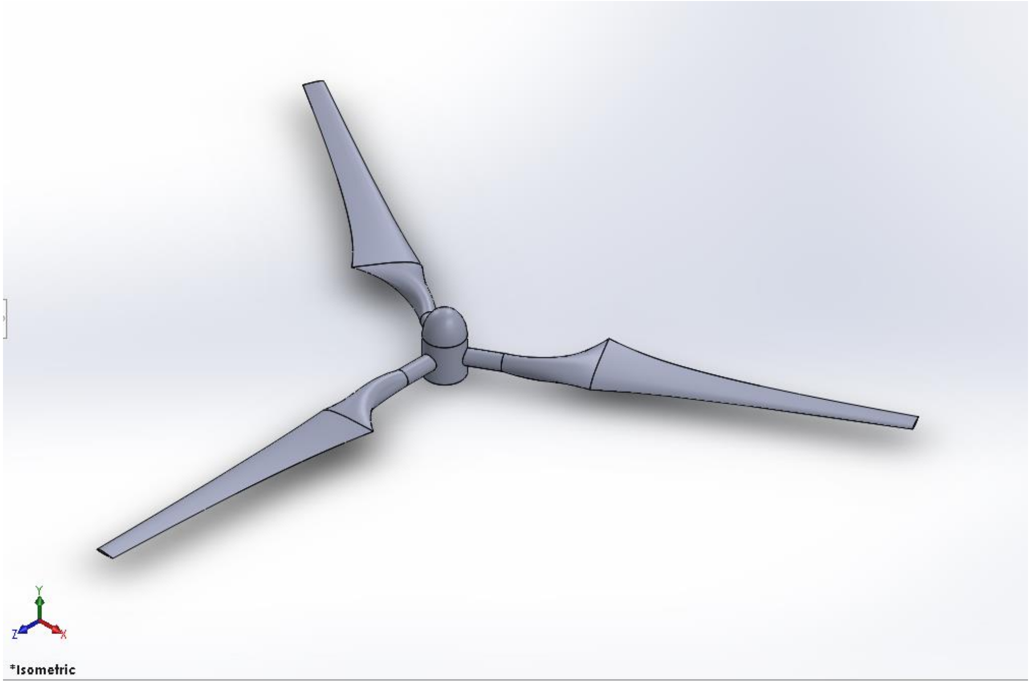

Figure 16: Designed Rotor Assembly

3.2.7 Numerical Analysis - CFD

The Numerical Analysis was done on ANSYS Fluent to determine the torque trends for the fluids acting on the turbine. Also, the visualization of fluid flow across the turbine was obtained. The values of C_L, C_D, and C_m were obtained which were to be used for structure analysis as they determine the lift and drag forces and moments which are detrimental for structure integrity.

3.2.7.1 Domain Specifications

The domain dimensions for each case (Wind and Water) were same. Only a few parameters were changed which will be specified later. There were two fluid domains in total:

i. Inner Fine Domain
ii. Outer Coarse Domain

3.2.7.1.1 Inner Fine Domain

Since this part of fluid is directly in contact with the turbine blades, this domain was supposed to be finer so that the calculations done were as accurate as possible. This domain was rotating (i.e., dynamic) to account for the rotation of the turbine blades.

3.2.7.1.2 Outer Coarse Domain

Outer Domain is the portion of fluid away from the turbine. Since this portion was not directly in contact with the turbine and didn't affect the calculations as such, we set it as coarse domain. The outer domain was set to be static.

Domain	**Shape**	**Dimensions**			
		Width (m)	**Height (m)**	**Length (m)**	**Diameter (m)**
Inner	Cylindrical	-	-	0.45	3.5
Outer	Cuboid	35	35	90	-

Table 07: Computational Domain Properties for CFD

3.2.7.2 Mesh Properties

The following table shows the final mesh sizes which yielded the desired results for our analysis:

Domain	Mesh Sizing	
	Body Sizing (m)	Face Sizing (m)
Inner Fine Domain	0.05	0.01
Outer Coarse Domain	2.00	0.01

Table 08: Mesh Sizing for CFD

3.2.7.3 Time Step Calculations

To Analyze properties at every 5^0 of rotation, we needed to find the value of time step to be used in the FLUENT Simulation setup. The analysis was done for a total of five consecutive resolutions of the turbine.

The time step calculations were done for both air-based and water-based analysis. The table below shows whole process for calculating the no. of time steps and the time step size for both water and wind analysis of turbine rotor:

Parameter	Wind	Water	Unit
RPM	300.848	49.118	rpm
RPS (=RPM/60)	5.014	0.8186	rps
Time for 1 Revolution	0.1994	1.2216	s
Time for 1^0 Rotation	5.5389×10^{-4}	3.393×10^{-3}	s
Time Step for 5^0	0.00277	0.016965	s
No. of Time Steps for 1 Revolution	72	72	$-$
No. of Time Steps for 5 Revolutions (Complete Analysis Time)	360	360	$-$

Table 09: Time Step Calculations for CFD

From the table it can be seen that to completely cover five complete revolutions of the rotor, the no. of time steps needed were 360 with step size of $5.5389 \times 10^{-4}\ s$ and $3.393 \times 10^{-3}\ s$ respectively for wind and water simulations.

3.2.7.4 ANSYS FLUENT Setup

Double precision was utilized to solve the model. For the simplification purposes due to limitations of computing resources the fluid flow was considered to ***incompressible*** in nature.

The transient flows are due to instabilities in the fluid and they are broadly categorized as following:

1. Naturally occurring transient flows
2. Forced transients

In our case the flow fell in the domain of *naturally occurring transient flow*. So, to account for that in the general setup of fluent, ***pressure-based*** solver with ***transient effects*** was enabled.

In the model setup of the fluent, the energy equation was left off, this can be done in pressure-based solver for incompressible flows as pressure work, kinetic energy and viscous dissipation i.e., thermal energy due to viscous shear are negligible. To account for turbulency ***Realizable k-ε model*** with ***standard wall functions*** was used.

In the material section of fluent, simulation was to be performed for two different fluids, the properties of fluid were specified. Constant values of density and dynamic viscosity were used as flow was assumed to be incompressible. The values used were same as used in analytical calculations in determining geometric parameters.

Then in cell zone condition section of fluent, fluid for both dynamic and stationary domains fluid was specified. Furthermore, for dynamic domain mesh motion was enabled. The rotation axis was specified as ***y-axis*** and the value of rotational velocity was assigned depending on which configuration was analysis being performed.

In the boundary condition section, inlet boundary condition was ***velocity inlet***, outlet boundary was ***pressure outlet*** and stationary domain side boundaries and turbine boundary were specified as ***walls***. Furthermore, a ***mesh interface*** was also generated between the faces of dynamic and stationary faces of the domain.

In the solution method, a ***coupled scheme*** was used with ***second order transient formulation***, ***second order turbulent kinetic energy***, ***first order upwind specific dissipation rate*** and ***first order upwind flow***. In the control section default values were left as it is.

Hybrid initialization was utilized with reference values taken from the inlet. In report definition section, drag, lift and moment coefficient monitors were generated. In the Run Calculation section ***fixed time stepping method*** was used. For every time step ***twenty iterations*** were specified. The calculations for time step have already been shown.

Parameter	**Specifications**
Precision	Double Precision
Fluid Flow	Incompressible
Fluid Flow	Naturally Occurring Transient Flow
Solver	Pressure based
Turbulence Model	$Realisable\ k - \varepsilon$
Wall Treatment	Standard
Axis of Rotation	y - axis
Inlet Boundary	Velocity Inlet
Outlet Boundary	Pressure Outlet
Transient Formulation	2^{nd} Order
Turbulent Kinetic Energy	2^{nd} Order
Upwind Specific Dissipation Rate	1^{st} Order
Upwind Flow	1^{st} Order
Initialization	Hybrid
Time Stepping Method	Fixed

Table 10: ANSYS FLUENT Setup

3.2.8 Numerical Analysis – Structural

In order to see the effects of fluid flow on the structure and get an idea of structural integrity, structural analysis was also performed. As the flow varied with time, so transient structure analysis was performed. One way coupling was utilized i.e., the results of Fluent were transferred to the Transient Structure setup to transfer the loads on the turbine due to fluid flow.

3.2.8.1 Analysis Setup

In the model section, a mesh of 0.025 m was generated. The rotation was applied to the turbine with an appropriate constraint at the turbine shaft. The analysis was run for around 1.5 seconds with a total of 1000 time steps. The equivalent strain, alternating stress due to fatigue, total deformation and factor of safety were evaluated.

The table below summarizes the setup details regarding structural analysis of the turbine:

Parameter	**Value**	**Unit**
Mesh Sizing	0.025	m
Analysis Time	1.5	s
No. of Time Steps	1000	$-$

Table 11: Rotor Structural Analysis - ANSYS Setup

3.2.8.2 Material Used

The material used for the structure analysis was ***Aluminum 2018 T61 Alloy***. This was selected as most of the turbines are made of Aluminum alloys and the purpose of the analysis was to just get the insight of structure integrity. Also, it is a light material, as the mass of our rotor is ***39.63 kg***. The properties of the alloy are as follow:

Property	**Value**	**Unit**
Tensile Yield Strength	317	MPa
Compressive Yield Strength	317	MPa
Tensile Ultimate Strength	421	MPa
Poisson Ratio	0.33	$-$
Density	2800	kg/m^3
Elastic Modulus	74.5	GPa

Table 12: Aluminum 2018 T61 Alloy Properties

3.3 Selection of the Electrical Components

3.3.1 Yaw control

Yaw control is a system that rotates the face of the turbine into the direction of the incoming fluid flow so that maximum torque can be acquired. Yaw control is used only in wind turbines because direction of fluid flow in case of wind changes while it remains same in case of water.

There are two types of yaw control:

3.3.1.1 Active yaw control

Active yaw control uses wind sensors that feed a control system, which in turn give signal to motors that rotate the nacelle of the turbine against the stationary base tower

3.3.1.2 Passive Yaw Control

Passive yaw control uses a tail fin that uses the impact of the incoming fluid to turn the turbine in the direction of the incoming fluid.

3.3.1.3 Yaw Control in Hybrid Turbine

We use ***passive yaw control*** in hybrid turbine because of following reasons:

- Passive yaw control is more economical compared with active yaw control
- In micro scale turbines, fin tails are more commonly used as they are effective and reliable
- Use of active yaw control causes difficulty in turbine portability due to increased weight

3.3.2 Current and Voltage Sensors

The current and voltage output of a hybrid turbine will vary depending upon fluid (air or water) and fluid velocity. Current and voltage sensors will be used to monitor the output of the turbine

3.3.3 Pitch Control

Pitch control allows the rotation of the blades so that a balanced fraction of the fluid energy can be extracted while keeping in check the maximum allowed safe limit of rotational speed. Pitch control uses a control system that sends signal to driving motors attached to turbine blades that adjust the pitch angle depending on the fluid speed and power output needed. In case of the hybrid turbine passive fixed pitch is used because

- It has small blade radius; the stresses are too low to incorporate active pitch control
- An active pitch control will make it economically non feasible due to the addition of driving motors, control system and sensors
- Adding driving motors for active pitch control will hinder turbine's portability

3.3.4 Generator Specifications

3.3.4.1 Selection Criteria

Following criteria was used to select generator,

- The generator should have a rated power in close proximity of the required target power
- The generator should have small size and less weight so that portability isn't compromised
- Permanent magnets are used in hydrokinetic turbine generator while wind turbine generator can use both electromagnets and permanent magnets, so the hybrid turbine generator should be of permanent magnet type

3.3.4.2 Selected Generator

The generator selected for our turbine is 145-STK-2M series permanent magnet alternator with a rated power of up to **1752 W**. The mass of the selected alternator is **6.2 kg**.

The alternator's technical details along with its comparison to other alternators are given below:

TECHNICAL CHARACTERISTICS
145 STK ALTERNATORS

See also the curves of Voltage, Torque, Efficiency vs Speed

			145STK2M		145STK4M		145STK6M		145STK8M	
	Rated speed	Rpm	650	1500	650	1500	650	1500	650	1500
Rated Power at Rated speed	Rated power (1)(2)	W	571	1752	1307	3389	1962	4904	2633	6462
	Input torque at rated speed(1)(2)	N.m	11.2	13.9	25.4	25.2	36	35.9	47.8	47
	Efficiency at rated power (1)(2)	%	75	81	76	86	81	87	81	88
	Current at rated power (1)	Amps	1.4	4.3	3.2	8	4.8	13	6.4	16
	Voltage at rated power (1)(2)(3)	V	244	250	243	260	246	231	249	248
Rated Power at Half speed	Rated Power at half speed (1)(2)	W	204	690	493	1566	739	2319	1075	3097
	Input torque at half speed (1)(2)	N.m	8.9	11.5	20.7	25.4	28.8	36	43.5	47.8
	Efficiency at half speed (1)(2)	%	68	77	70	78	76	82	73	83
	Number of poles (number of pairs of poles)		12 (6)							
	Cogging torque	N.m	0.2		0.4		0.6		0.8	
	Phase résistance at 20°C	Ohm	19.8	4.53	8.6	1.4	4.11	0.59	3.18	0.51
	Phase inductance (5)	mH	105	24	60	10	34	4.9	25.8	4.1
	Voltage at no load (back emf) at 20°C (4)	V	365	393	390	367	357	312	361	334
	Rotor inertia	10^{-3} Kg.m2	1.28		2.24		3.19		4.14	
	Weight	Kg	6.2		10.4		14.5		18.7	
	Power cable square section (6)	mm²	4x1.5		4x1.5		4x1.5		4x1.5	
	Power cable diameter	mm	Ø8.6		Ø8.6		Ø8.6		Ø8.6	

Figure 17: 145 STK Alternators - Specifications

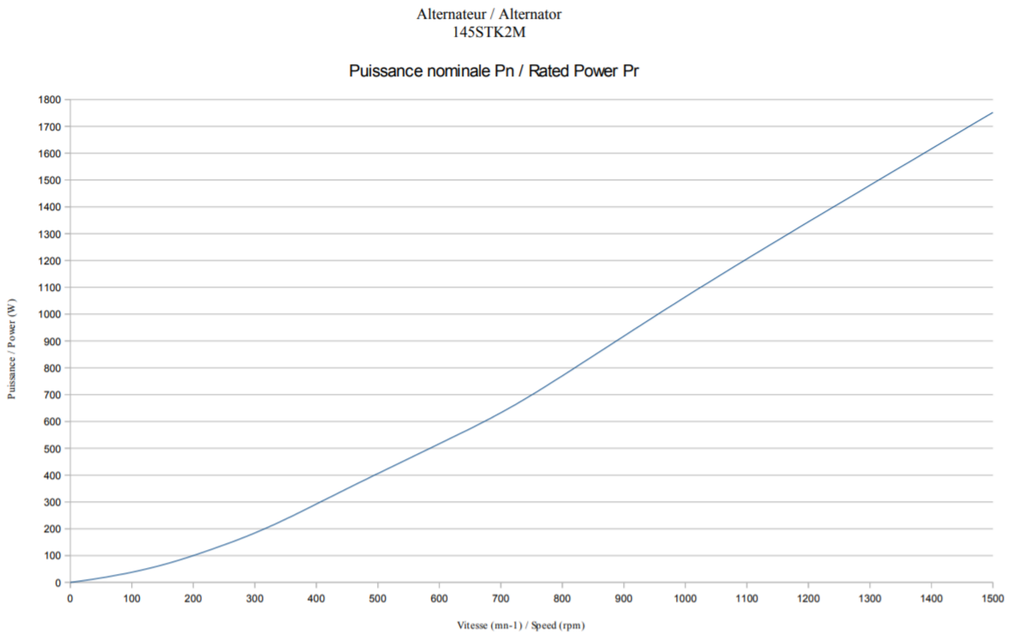

Figure 18: 145STK-2M Alternator - Power vs RPM

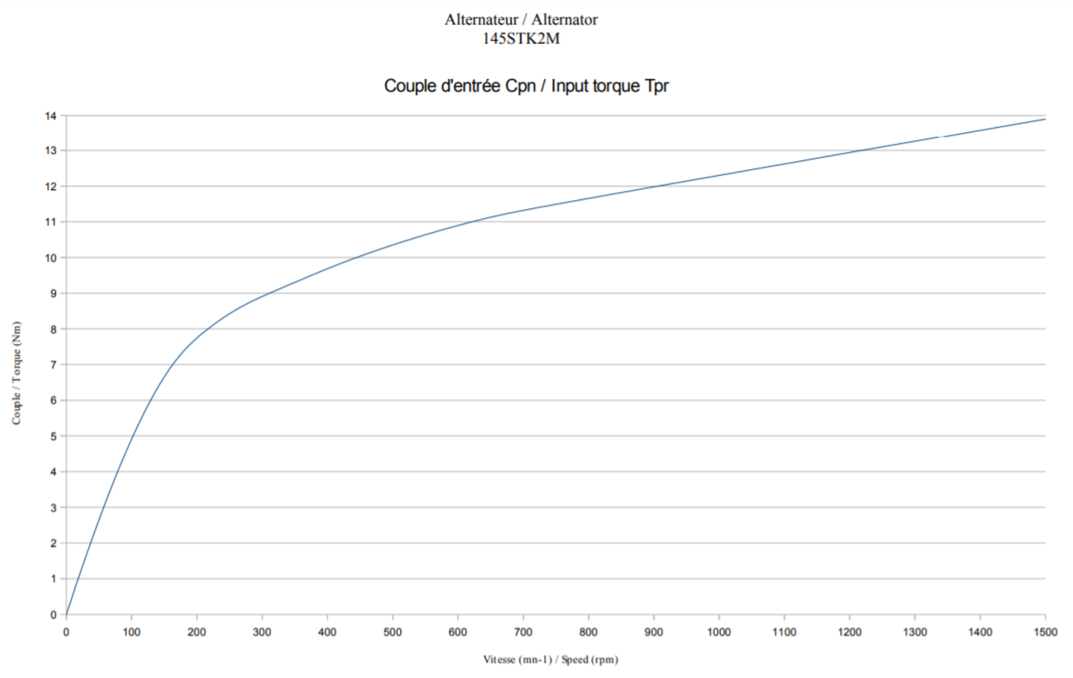

Figure 19: 145STK-2M Alternator - Torque vs RPM

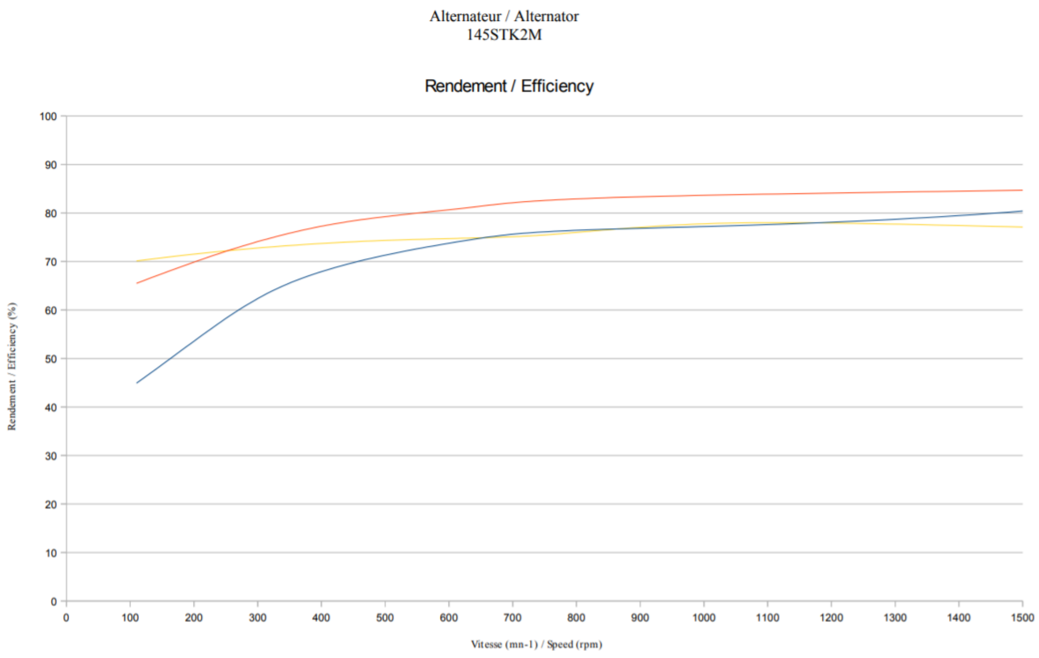

Figure 20: 145STK-2M Alternator - Efficiency vs RPM

From the above data FOR 145STK-2M Alternator, for a rated power of 1000 watt:

- The RPM is around 960
- Torque is around 12.2 N.m.
- Efficiency is around 77.2%

The parameters are summarized as a table below:

Sr. No.	Parameters (for 1000 W Output)	Value	Unit
1.	RPM	958.780	rpm
2.	Torque	12.181	$N-m$
3.	Mass	6.200	kg
4.	Efficiency	77.180	%

Table 13: 145STK-2M Characteristics at 1000W Output

3.4 Transmission Systems

The generators used in wind turbines and hydrokinetic turbines have RPMs of about 800 rpm that may go up to as much as 1500 rpm . The rotor blades in wind have about 300.848 rpm and rotor blades had about 49.118 rpm in water. So, a gear transmission system is needed to increase the RPM and decrease the torque transmitted from the turbine.

3.4.1 Gear Transmission System in Hybrid Turbine

We had to address following challenges to design a gear transmission system for hybrid turbine:

- Increase the RPM and decrease the torque for both water and wind media.
- Propose a mechanism for achieving two different gear ratios for wind – generator, and water – generator configurations.

3.4.2 Steps in Designing Gear Transmission System

Following approach was used to come up with design for transmission system

- RPMs for wind and water medium were calculated from the typical values of TSR. RPM for water medium was 49.118 rpm and RPM for wind medium was 300.848 rpm

Parameter	Wind	Water	Generator
RPM	300.848	49.118	960

Table 14: Rotor and Generator RPM

- RPM for 1000 Watt Rated power for generator was 960, obtained from the technical characteristics chart for a generator
- The gear ratios for water – generator, and wind – generator was obtained from the RPMs for wind, water and generator
- The criteria used for determining gear ratio was to restrict gear ratio to below 10 to ensure smooth functioning of gears. We had gear ratio of 18.75 for water medium so we had to introduce an intermediate shaft and compound two stage gear system to make sure that gear ratio stayed below 10.
- The gear teeth for rotor shaft for wind / water and gear teeth for generator shaft were determined from respective gear ratios.
- After multiple iterations, we decided on using a single gear of 300 gear teeth on the main rotor shaft, two gears of 75 gear teeth and 36 gear teeth on the intermediate shaft for water and wind mediums respectively. Lastly, there were 16 gear teeth and 94 gear teeth on the generator shaft for water and wind mediums respectively.

- ***1.7 mm*** gear module was used.

The table below shows the specifications of the gears used in the transmission system for both wind and water configurations:

Working Fluid	**Main Shaft**	**Intermediate Shaft**	**Generator Shaft**	**Achieved Torque Reduction**
Water	300 teeth	75 teeth	16 teeth	18.75
Wind	300 teeth	36 teeth	94 teeth	3.2

Table 15: Transmission System Specifications

3.4.3 CAD Model for Transmission Assembly

In the following CAD model, the 300 teeth larger gear can be seen on the right main rotor shaft and two gears on each intermediate and generator shaft for wind and water mediums. The larger rotor gear can change its position to achieve two different gear ratios for wind and water.

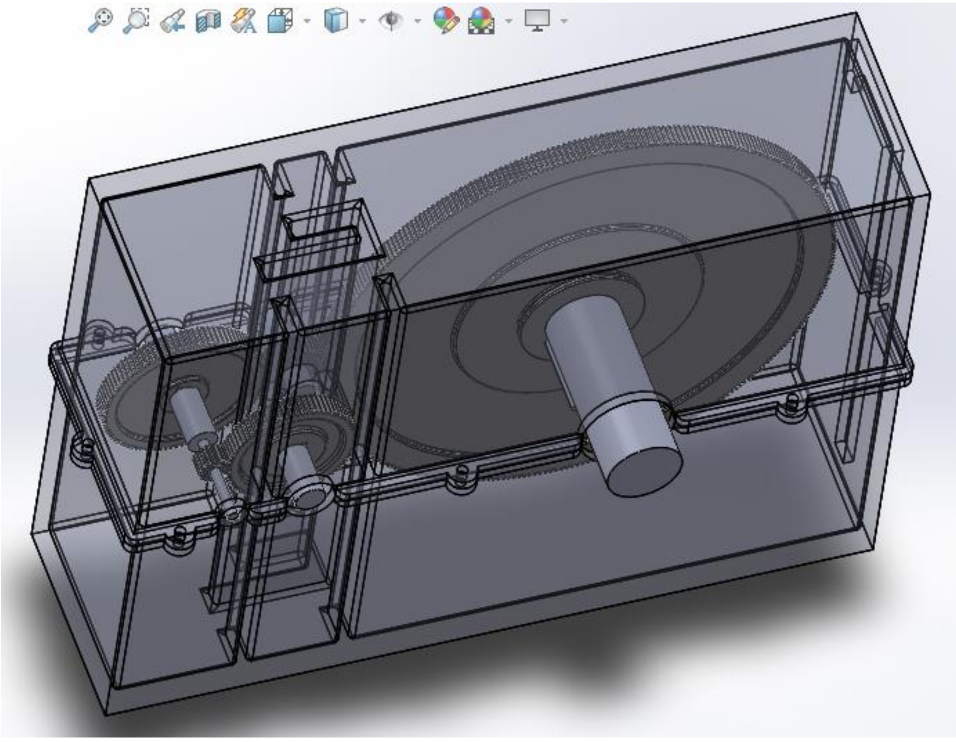

Figure 21: CAD Model for Transmission Assembly

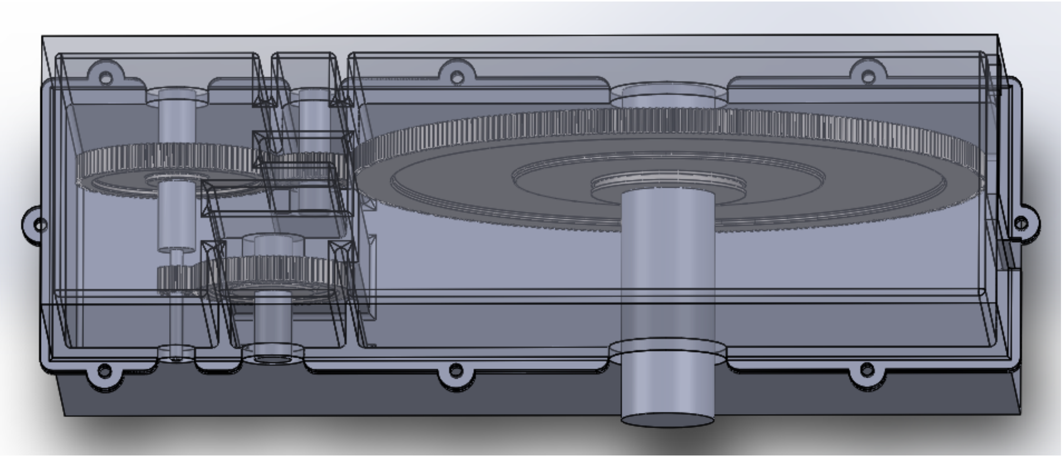

Figure 22: Transmission System – Wind Configuration

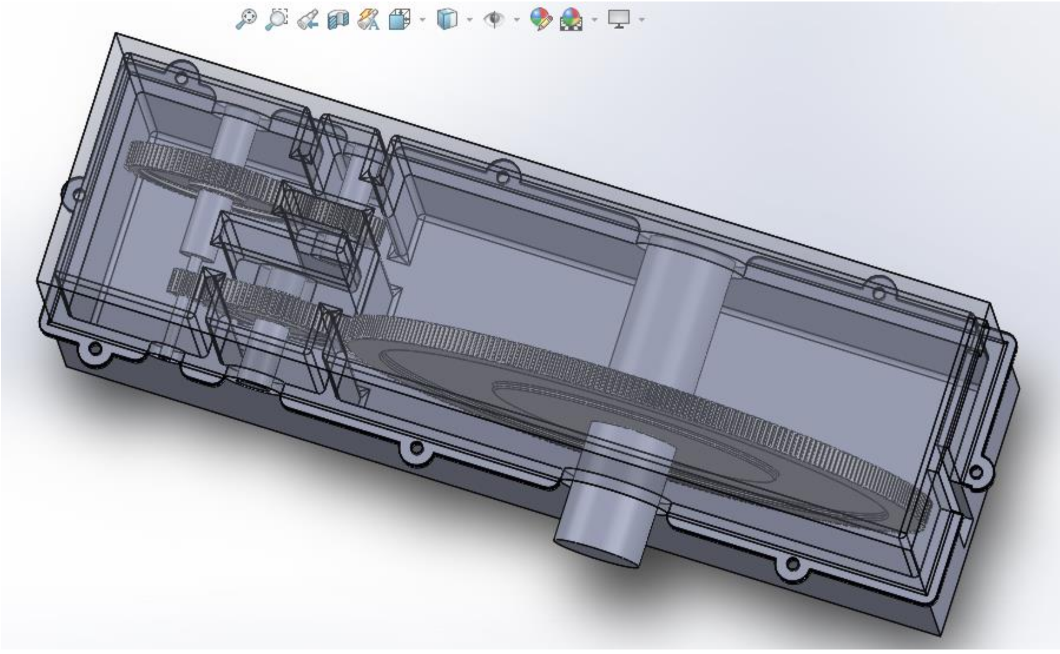

Figure 23: Transmission System – Water Configuration

4 RESULTS & DISCUSSIONS

In this chapter, we will show and discuss meaning of the results obtained for both the Structural and Computational Fluid Dynamics (CFD) Analysis done for our various components of Turbine.

4.1 Computational Fluid Dynamics

After applying the conditions explained in Chapter 03, the analysis was carried out in the ANSYS Fluent separately for both the media (i.e., air and water). The purpose was to obtain velocity contours of the moving fluid around the turbine to get an understanding of the fluid flow around the blades. Also, for the calculation of power from simulation, torque was obtained. The results obtained for wind and water simulations will be discussed one by one.

4.1.1 Wind Simulation Results

The results obtained for the wind simulation are discussed below:

4.1.1.1 Velocity Vectors

For wind Simulation, velocity vectors that were obtained are shown below:

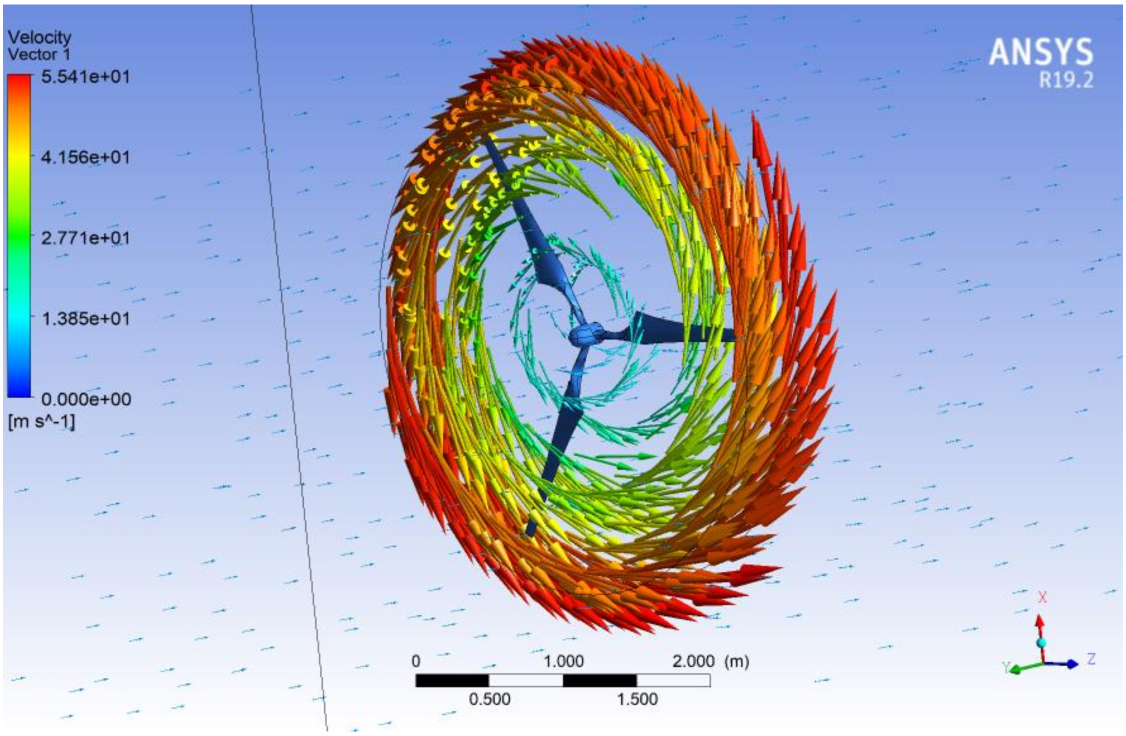

Figure 24: CFD Wind - Velocity Vectors

From the figure showing fluid velocity vectors around the turbine cavity, it can be seen that the maximum tangential velocity of fluid is obtained near the tips of the blades along the outer circumference of the turbine rotor with a maximum value of $55.41\ m/s$. The fluid velocity is near zero at the axis of rotation and gradually increases along the radius till it reaches the tip and few inches beyond.

4.1.1.2 Velocity Contours

The velocity contours obtained for the respective planes are shown below:

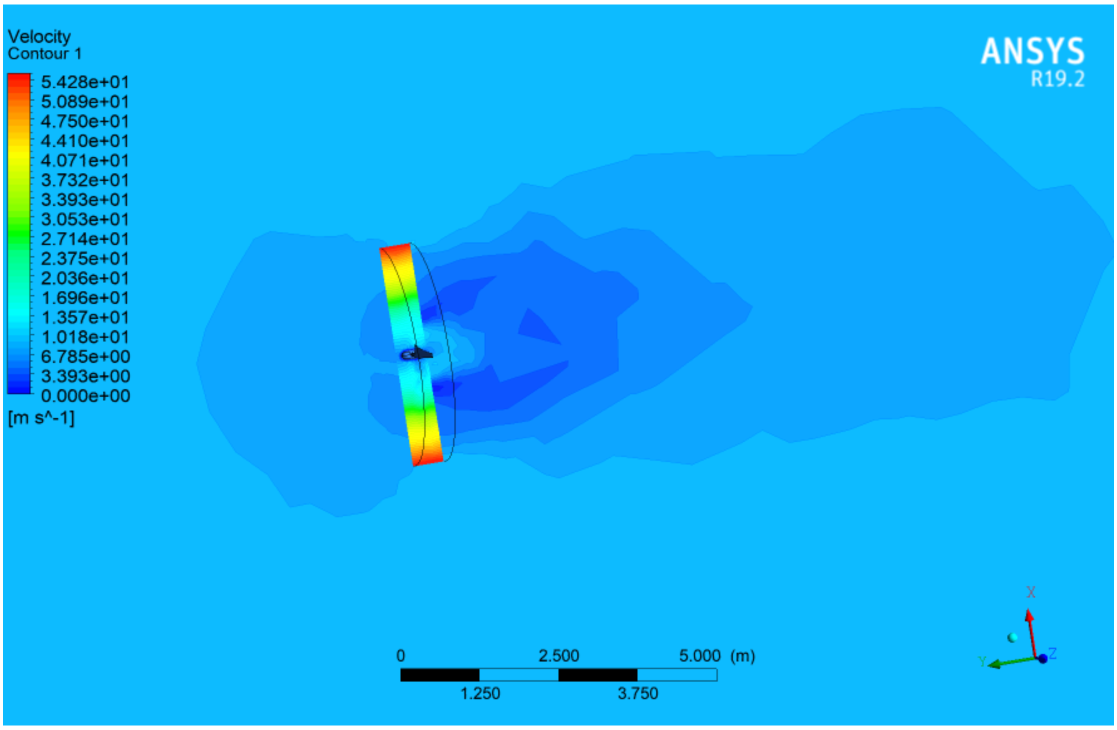

Figure 25: CFD Wind - Velocity Contours 01

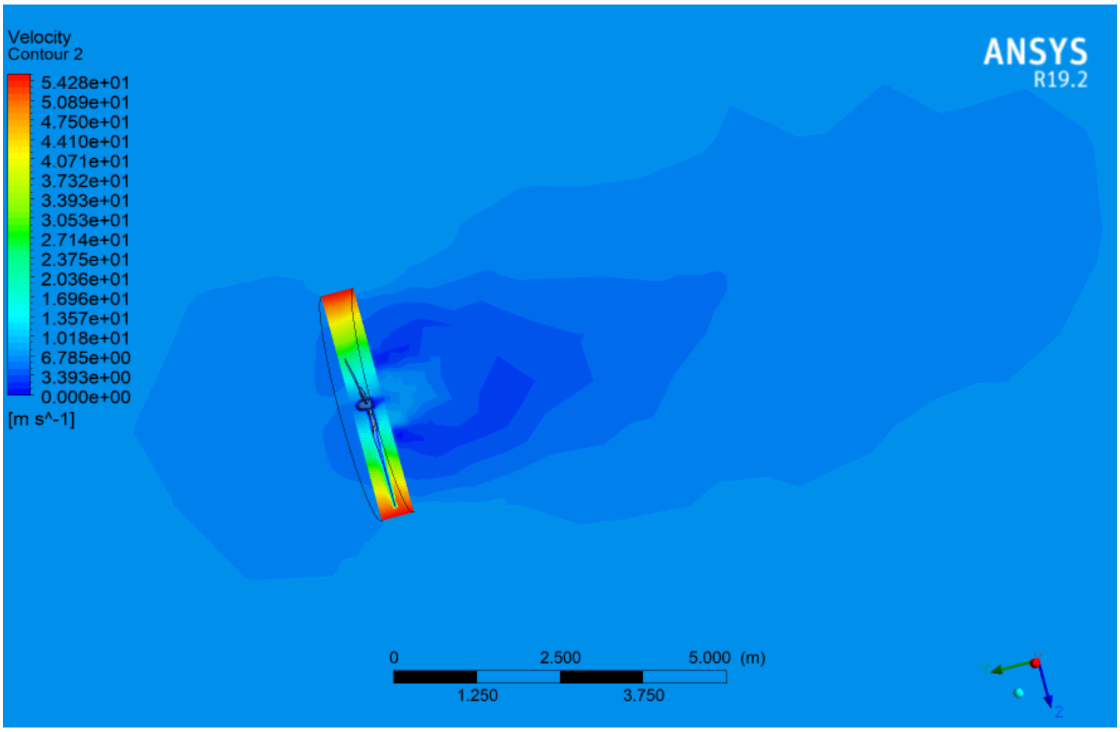

Figure 26: CFD Wind - Velocity Contours 02

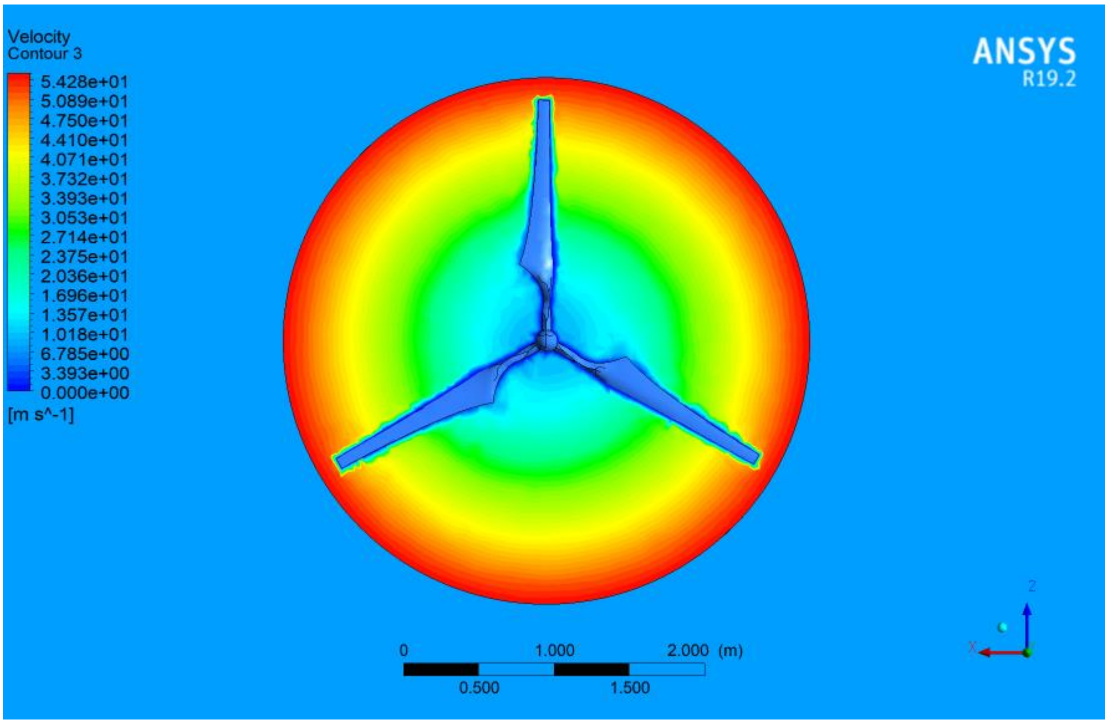

Figure 27: CFD Wind - Velocity Contours 03

From the velocity contours obtained through CFD post-processor, it can be seen that the velocity of fluid ranges from $0\ m/s$ at the center to $54.28\ m/s$ at the edges of the rotating cylindrical fluid domain.

4.1.1.3 Fluid Streamlines

To observe the fluid flow pattern, it's necessary to have a look at the fluid streamlines to have a grasp of how the fluid flows in the presence of turbine. The figure below shows the fluid streamlines as the turbine rotates in the air:

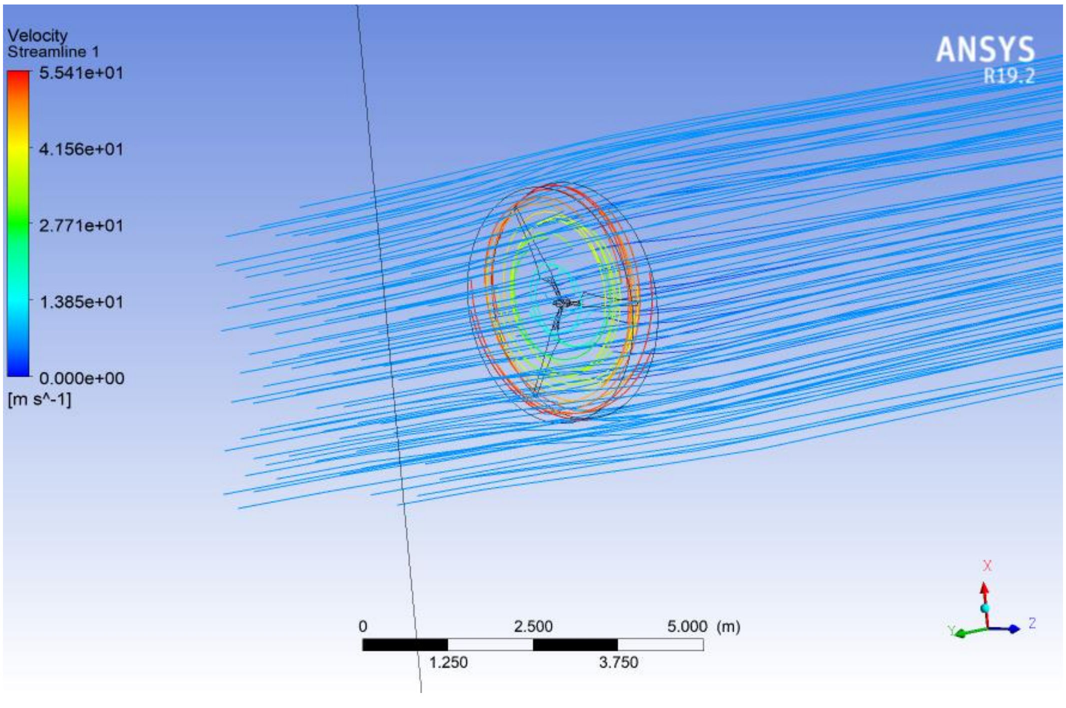

Figure 28: CFD Wind - Fluid Streamlines

4.1.1.4 Tip Average Velocity

In order to confirm the value of TSR that we used in calculations, the value of velocity at the blade tip was required. This value was calculated by forming a velocity vector at the blade tip in the Post-CFD Processor after completion of simulations.

The figure below shows the velocity vector profile at the blade tip:

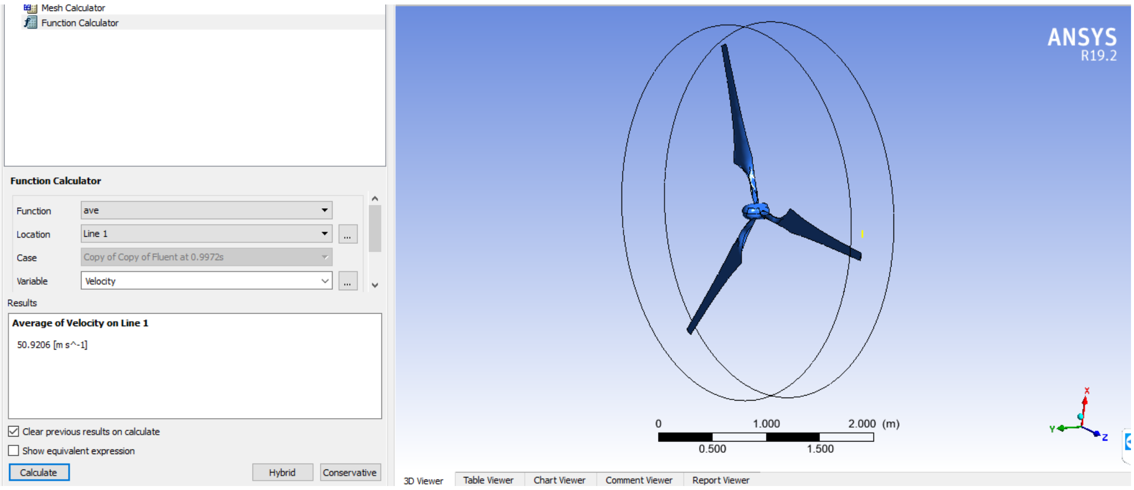

Figure 29: CFD Wind - TSR Verification

From the figure it can be seen that:

$$Velocity\ at\ Tip = 50.9206\ m/s$$

On the other hand,

$$Wind\ Stream\ Velocity = 7.0\ m/s$$

Dividing these values to get the numerical TSR:

$$\Rightarrow Achieved\ TSR = \frac{50.9206}{7.0} = 7.2744$$

Also,

$$Initially\ assumed\ TSR = 7$$

Which means that our initial assumptions for the TSR match with the value of TSR obtained from the CFD Analysis.

4.1.1.5 Torque and Power Calculations

We also needed the value of torque produced by the turbine under the given assumptions and conditions. The reason being the power production capacity of the turbine can be calculated from the value of torque it produces. In this way, we would be able to find out whether the turbine was capable of producing the power it was required to produce under the given conditions or not. The results could be compared with the analytical ones from MATLAB.

The figure followed shows the torque obtained for the turbine in case of air from the ANSYS Fluent CFD Post-Processor:

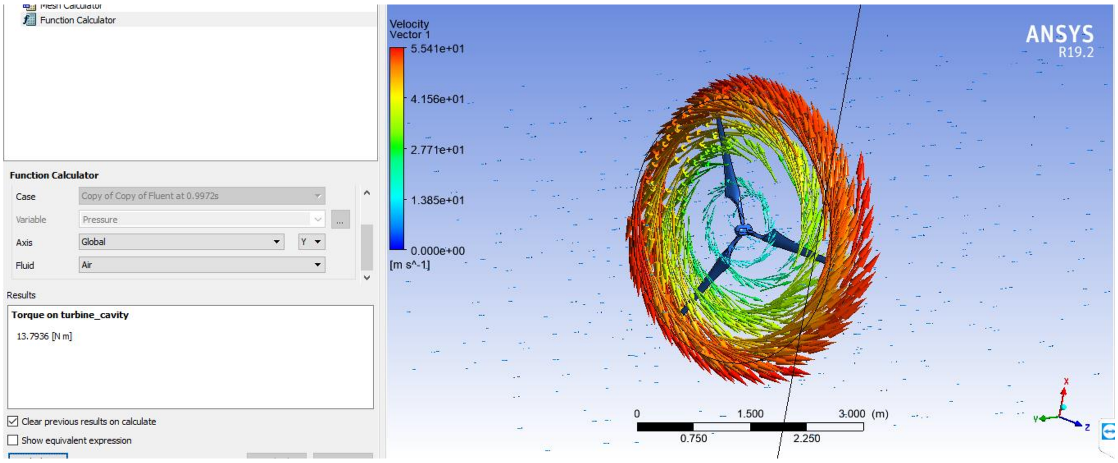

Figure 30: CFD Wind – Torque and Power Calculations

We can see that the value of torque obtained for our turbine under the set conditions for the wind case is 13.7936 $N - m$.

Now, to calculate the power produced, the product of the achieved torque and the angular velocity was taken as shown:

$$Achieved\ Torque = 13.7936\ N - m$$

$$Angular\ Velocity = 31.505\ rad/s$$

$$\Rightarrow Power\ Produced = 13.7936\ \times 31.505 = 434.5674\ W$$

The power produced in case of wind configuration was 434.5674 W. Our minimum requirement for the power produced was 500 W which means that the achieved power output was in close range of our minimum desired output.

Calculating percentage difference:

$$\frac{500 - 434.5674}{500} \times 100\ \% = 13.086\ \%$$

Thus, the power achieved was 13.086 % less than that of the desired power output.

4.1.2 Water Simulation Results

The results obtained for the water simulation are discussed below:

4.1.2.1 Velocity Vectors

For water Simulation, velocity vectors that were obtained are shown below:

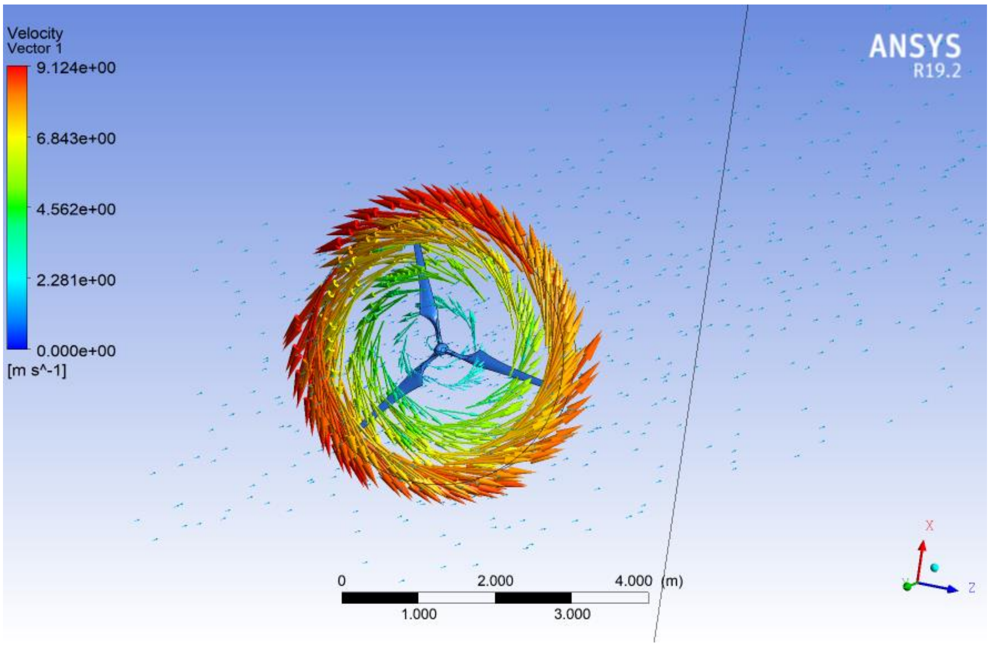

Figure 31: CFD Water - Velocity Vectors

From the figure showing fluid velocity vectors around the turbine cavity, it can be seen that the maximum tangential velocity of fluid is obtained near the tips of the blades along the outer circumference of the turbine rotor with a maximum value of $9.124\ m/s$. The fluid velocity is near zero at the axis of rotation and gradually increases along the radius till it reaches the tip and few inches beyond.

4.1.2.2 Velocity Contours

The velocity contours obtained for the respective planes are shown below:

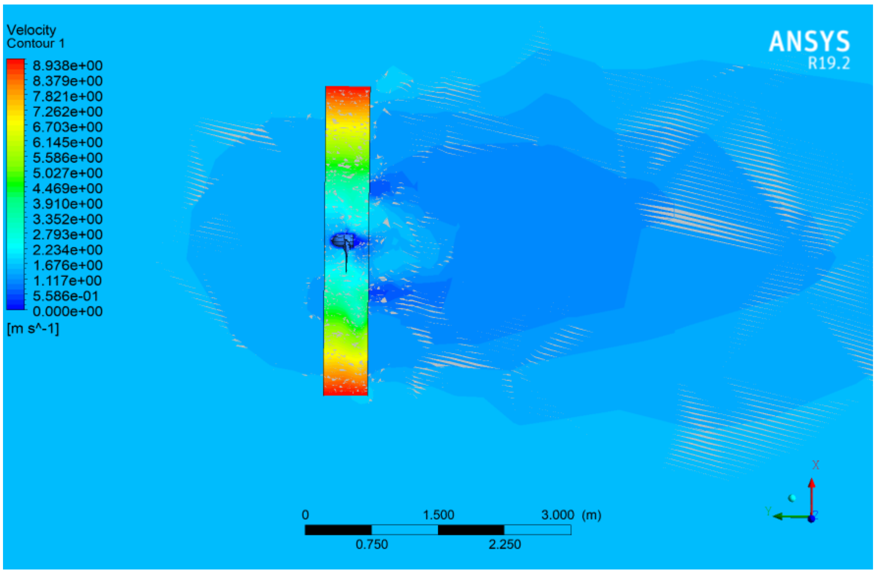

Figure 32: CFD Water - Velocity Contours 01

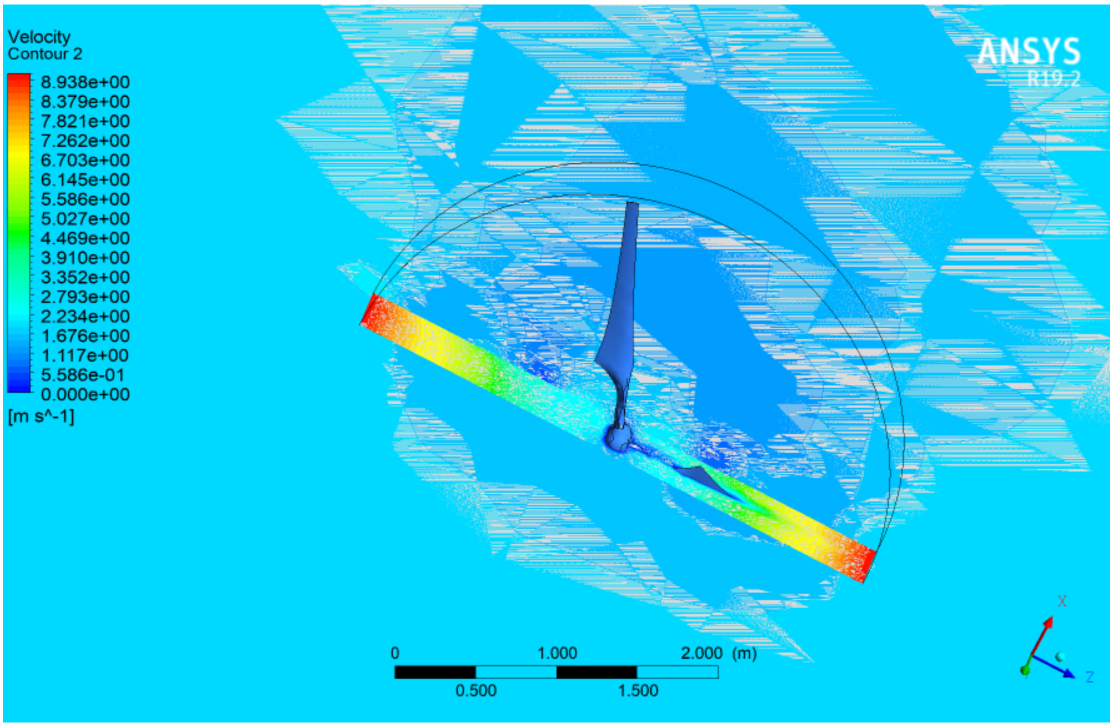

Figure 33: CFD Water - Velocity Contours 02

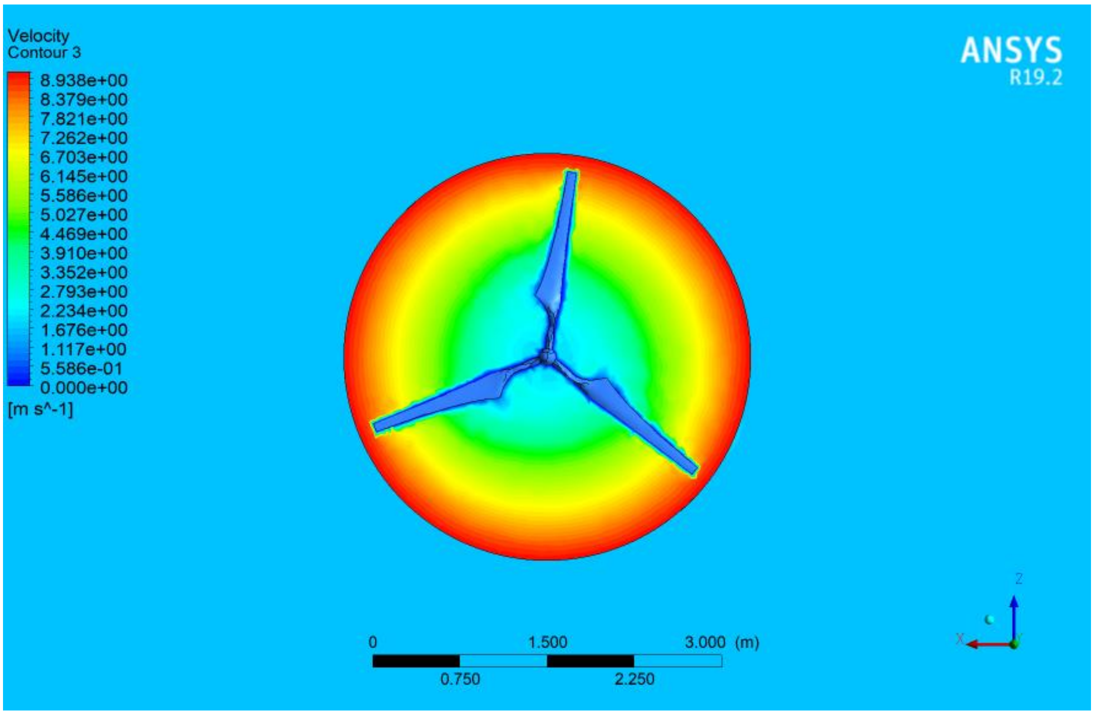

Figure 34: CFD Water - Velocity Contours 03

From the velocity contour picture obtained through CFD post-processor, it can be seen that the velocity of fluid ranges from 0 m/s at the center to 8.938 m/s at the edges of the rotating cylindrical fluid domain.

4.1.2.3 Fluid Streamlines

To observe the fluid flow pattern, it's necessary to have a look at the fluid streamlines to have a grasp of how the fluid flows in the presence of turbine. The figure below shows the fluid streamlines as the turbine rotates in the water:

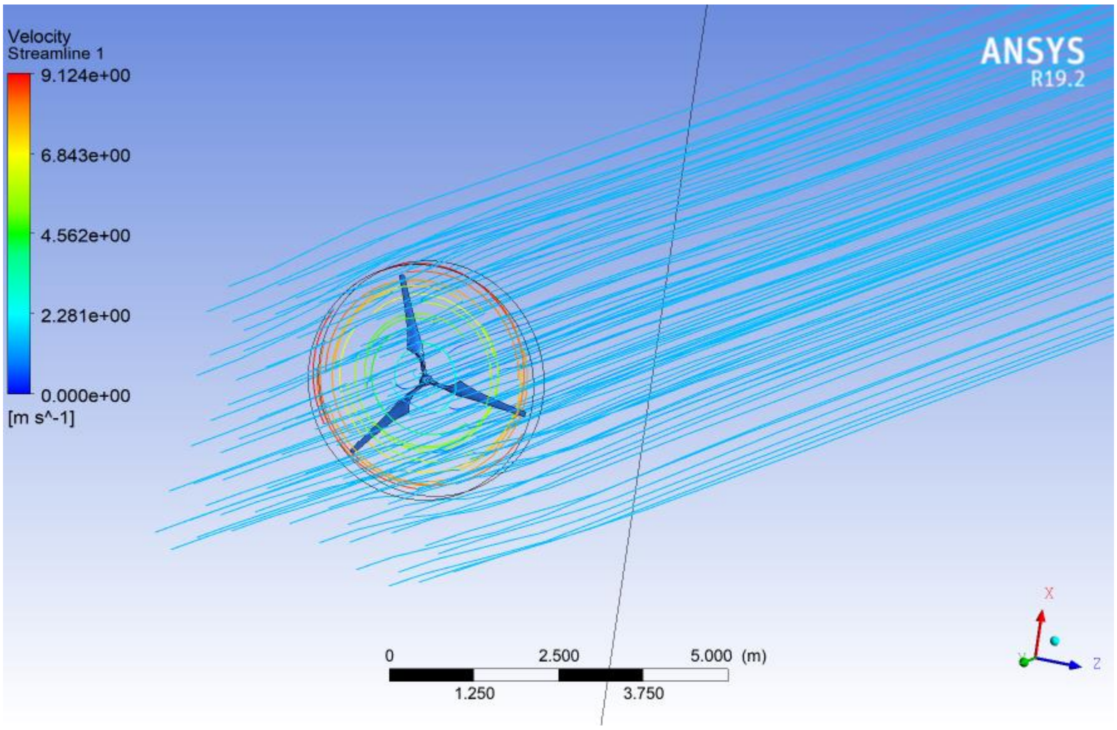

Figure 35: CFD Water - Fluid Streamlines

4.1.2.4 Tip Average Velocity

In order to confirm the value of TSR that we used in calculations, the value of velocity at the blade tip was required. This value was calculated by forming a velocity vector at the blade tip in the Post-CFD Processor after simulations.

The figure below shows the velocity vector profile at the blade tip:

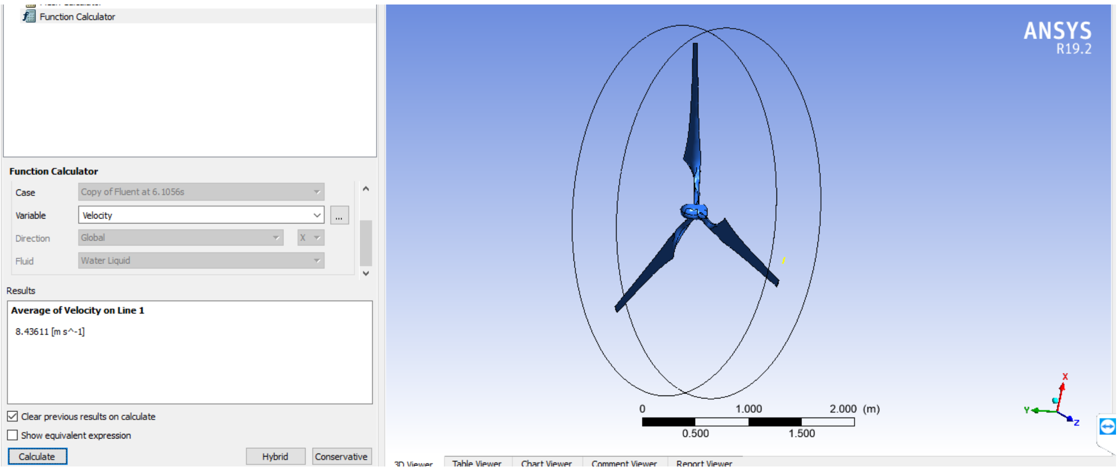

Figure 36: CFD Water - TSR Verification

From the figure it can be seen that:

$$Velocity\ at\ Tip = 8.43611\ m/s$$

On the other hand,

$$Water\ Stream\ Velocity = 1.6\ m/s$$

Dividing these values to get the numerical TSR:

$$\Rightarrow Achieved\ TSR = \frac{8.43611}{1.6} = 5.2726$$

Also,

$$Initially\ assumed\ TSR = 5$$

Which means that our initial assumptions for the TSR match with the value of TSR obtained from the CFD Analysis.

4.1.2.5 Torque and Power Calculations

We also needed the value of torque produced by the turbine under the given assumptions and conditions. The reason being the power production capacity of the turbine can be calculated from the value of torque it produces. In this way, we would be able to find out whether the turbine was capable of producing the power it was required to produce under the given conditions or not. The results could be compared with the analytical ones from MATLAB.

The figure followed shows the torque obtained for the turbine in case of water from the ANSYS Fluent CFD Post-Processor:

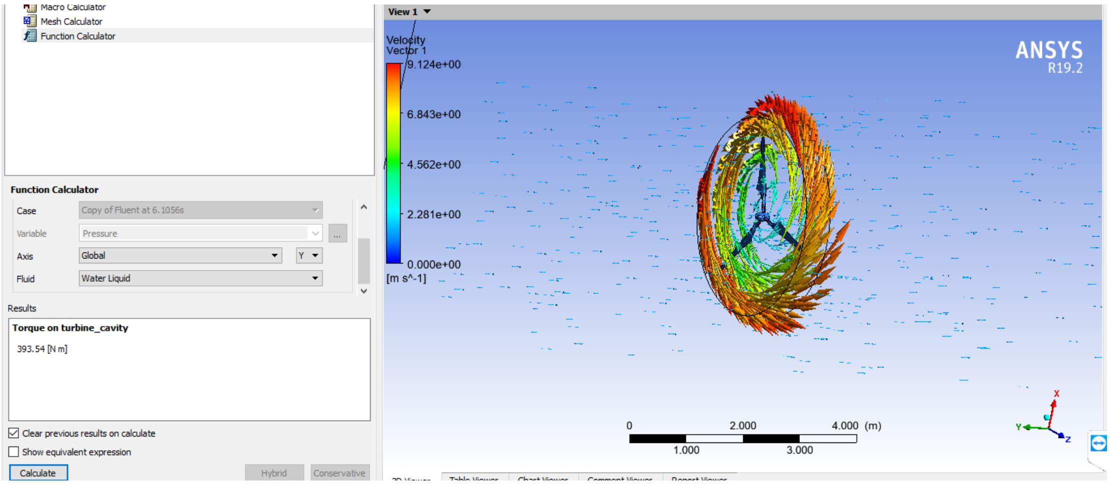

Figure 37: CFD Water - Torque and Power Calculations

We can see that the value of torque obtained for our turbine under the set conditions for the wind case is $393.54\ N - m$.

Now, to calculate the power produced, the product of the achieved torque and the angular velocity was taken as shown:

$$Achieved\ Torque = 393.54\ N - m$$

$$Angular\ Velocity = 5.144\ rad/s$$

$$\Rightarrow Power\ Produced = 393.54\ \times 5.144 = 2024.3698\ W$$

Thus, the power produced in case of water configuration was $2024.3698\ W$. Our maximum requirement for the power produced was $1000\ W$ which means that the achieved power output was more than double of our maximum desired output.

$$\frac{2024.3698 - 1000}{1000} \times 100\ \% = 102.437\ \%$$

Thus, the power achieved was $102.437\ \%$ more than that of desired power output.

4.2 Structural Analysis

After performing the CFD Analysis on the turbine rotor for Power and Torque Calculations, the structural analysis was done on the rotor as well as the Gear Assemblies for Wind and Water Configurations.

The main purpose was to understand whether these components would withstand the stresses acting upon them or not. If they withstood the stresses, the Factor of Safety was calculated for these components using ANSYS Mechanical.

4.2.1 Rotor Structural Analysis – Wind

First, structural analysis of rotor was done by importing the pressure profiles on the rotor from the CFD Post and then running the Transient Structural Analysis on the Turbine Rotor. The Process Results are discussed below:

4.2.1.1 Imported Pressure Profiles

The Pressure Distribution Contours for the rotor blades in case of wind configuration, imported from the CFD Analysis of the rotor, are shown below:

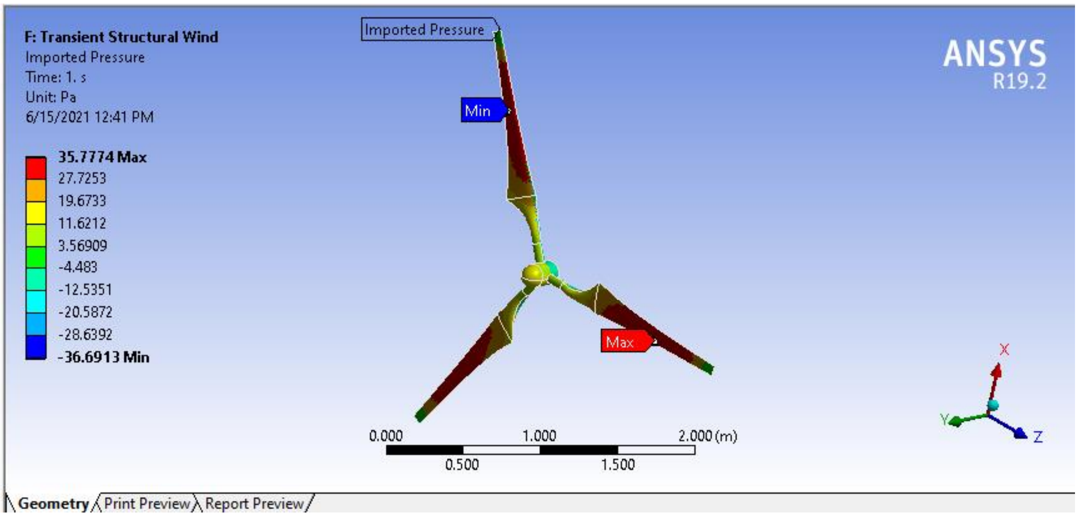

Figure 38: Rotor Structural Analysis (Wind) - Imported Pressure Distributions

4.2.1.2 Equivalent Alternating Stress

The figure below shows the Equivalent Alternating Stress on the Rotor due to the wind pressure obtained through Structural Analysis:

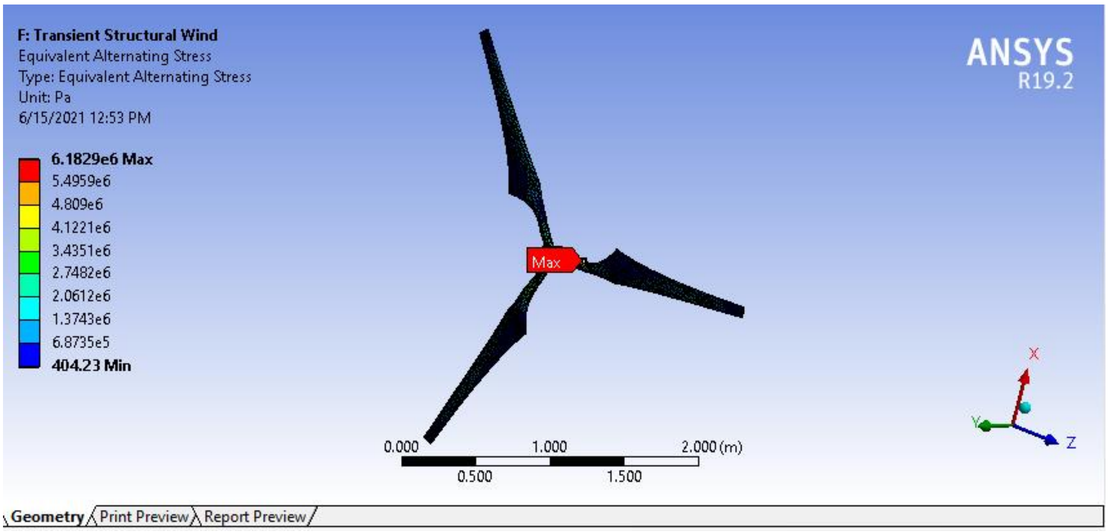

Figure 39: Rotor Structural Analysis (Wind) - Equivalent Alternating Stress

From the figure, the maximum Equivalent Alternating Stress on the Rotor Profile was observed to be 6.1829 MPa. This value is far less than the yield strength of the material that we selected i.e., 317 MPa.

4.2.1.3 Equivalent Elastic Strain

Similarly, the equivalent elastic strain on the rotor in case of wind configuration is shown as:

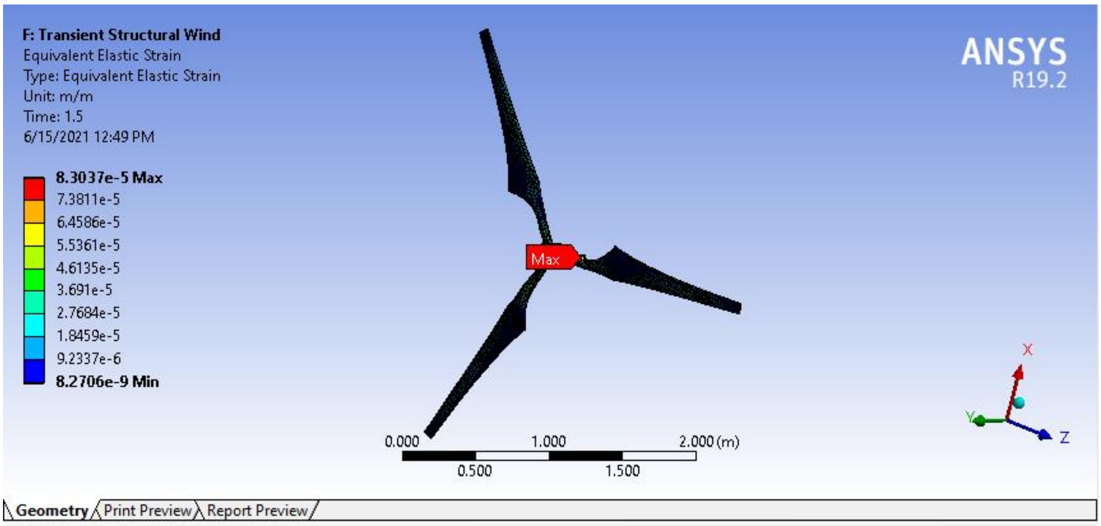

Figure 40: Rotor Structural Analysis (Wind) - Equivalent Elastic Strain

From the figure, the maximum value for Equivalent Elastic Strain on the rotor in case of wind was found to be 8.3037×10^{-5}.

4.2.1.4 Total Deformation

The figure below shows the Total Deformation of the turbine rotor in wind configuration:

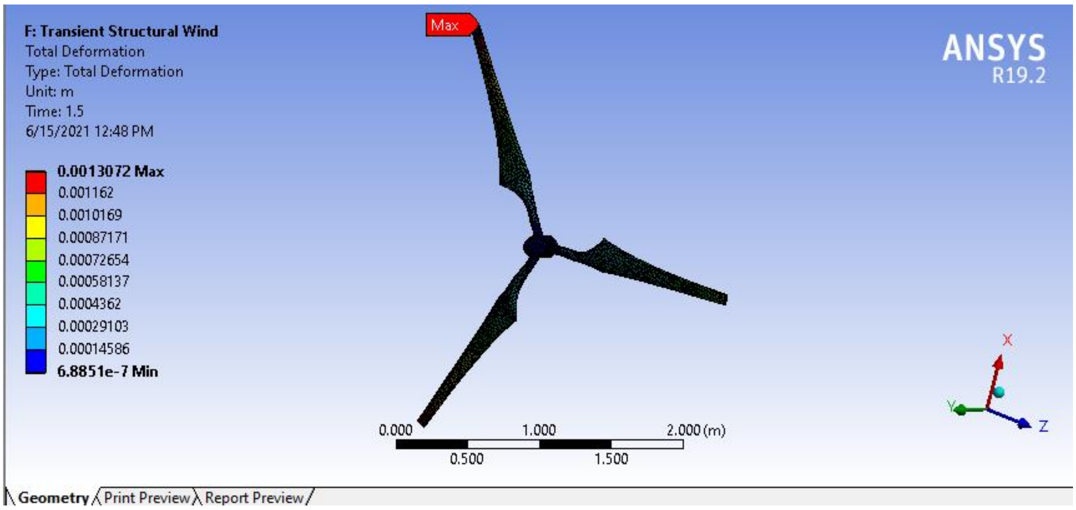

Figure 41: Rotor Structural Analysis (Wind) - Total Deformation

From the figure, the maximum value for Total Deformation on the rotor in case of wind was found to be $0.0013072\ m$.

4.2.1.5 Factor of Safety

The figure below shows the Factor of Safety for Rotor in case of Wind Configuration obtained from the Structural Analysis:

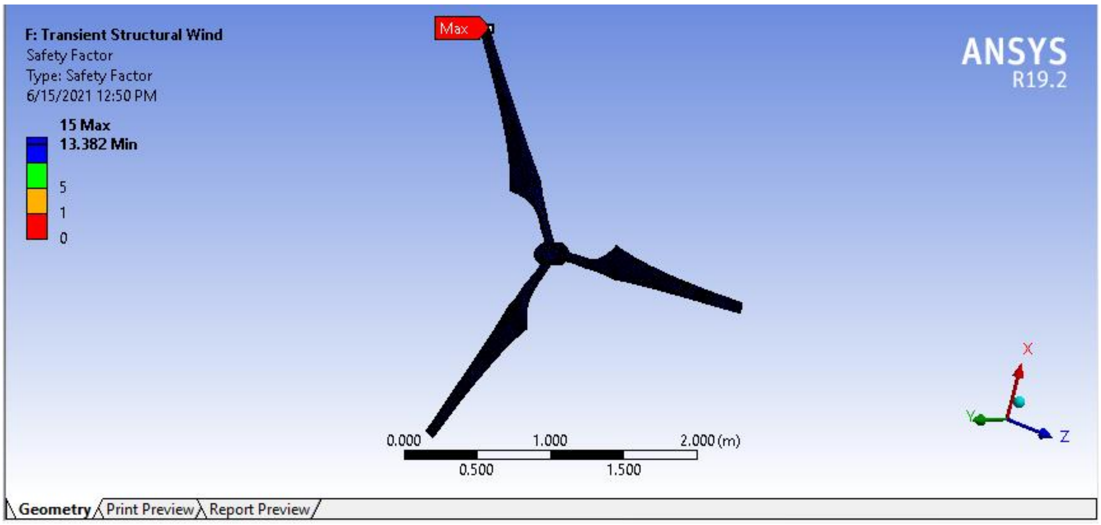

Figure 42: Rotor Structural Analysis (Wind) - Factor of Safety

From the figure, the minimum factor of safety obtained for rotor in wind configuration was:

$$Minimum\ FoS_{wind} = 13.382$$

Which means that the rotor is too safe for any type of transient stresses acting on it due to wind.

4.2.2 Rotor Structural Analysis – Water

First, structural analysis of rotor was done by importing the pressure profiles on the rotor from the CFD Post and then running the Transient Structural Analysis on the Turbine Rotor. The Process Results are discussed below:

4.2.2.1 Imported Pressure Profiles

The Pressure Distribution Contours for the rotor blades in case of water configuration, imported from the CFD Analysis of the rotor, are shown below:

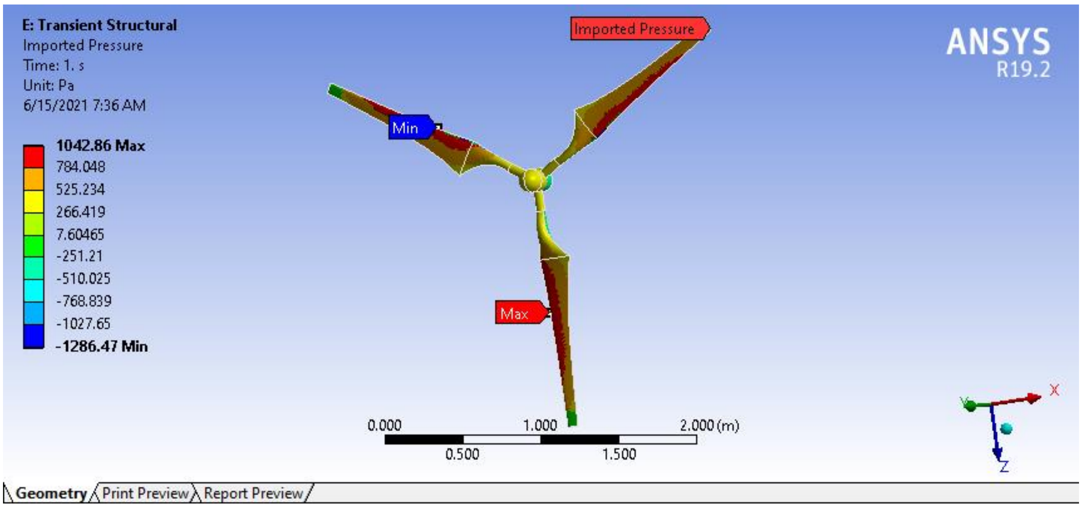

Figure 43: Rotor Structural Analysis (Water) - Imported Pressure Distributions

4.2.2.2 Equivalent Alternating Stress

The figure below shows the Equivalent Alternating Stress on the Rotor due to the water pressure obtained through Structural Analysis:

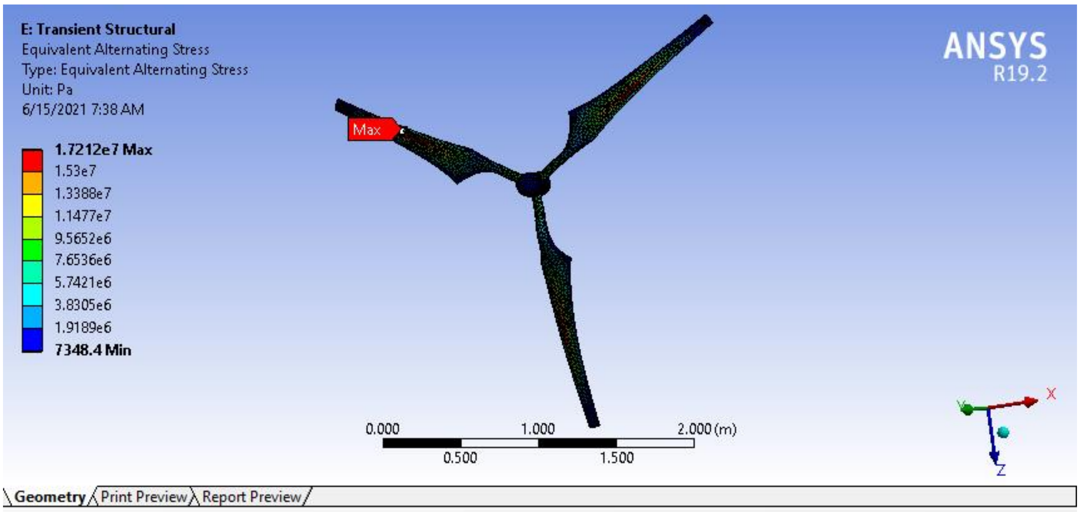

Figure 44: Rotor Structural Analysis (Water) - Equivalent Alternating Stress

From the figure, the maximum Equivalent Alternating Stress on the Rotor Profile was observed to be 17.212 MPa. This value is far less than the Yield Strength of the material that we selected i.e., 317 MPa .

4.2.2.3 Equivalent Elastic Strain

Similarly, the equivalent elastic strain on the rotor in case of water configuration is shown as:

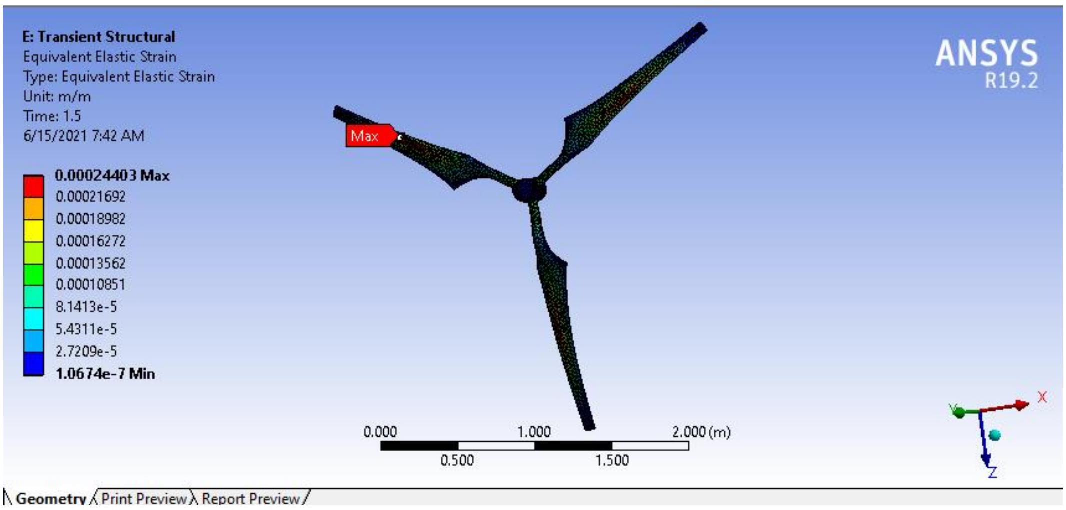

Figure 45: Rotor Structural Analysis (Water) - Equivalent Elastic Strain

From the figure, the maximum value for Equivalent Elastic Strain on the rotor in case of water was found to be 2.4403×10^{-4}.

4.2.2.4 Total Deformation

The figure below shows the Total Deformation of the turbine rotor in water configuration:

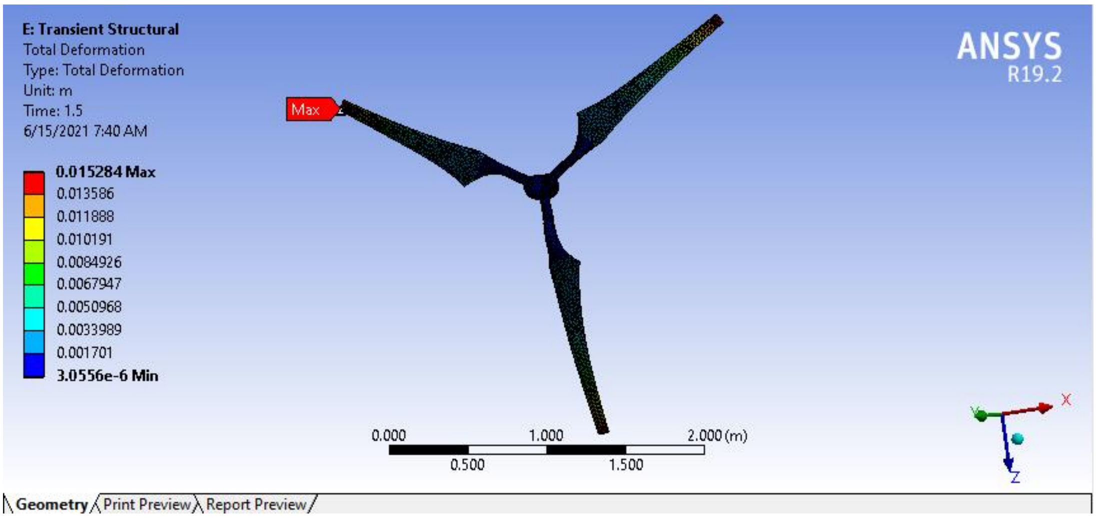

Figure 46: Rotor Structural Analysis (Water) - Total Deformation

From the figure, the maximum value for Total Deformation on the rotor in case of water was found to be $0.015284\ m$.

4.2.2.5 Factor of Safety

The figure below shows the Factor of Safety for Rotor in case of Water Configuration obtained from the Structural Analysis:

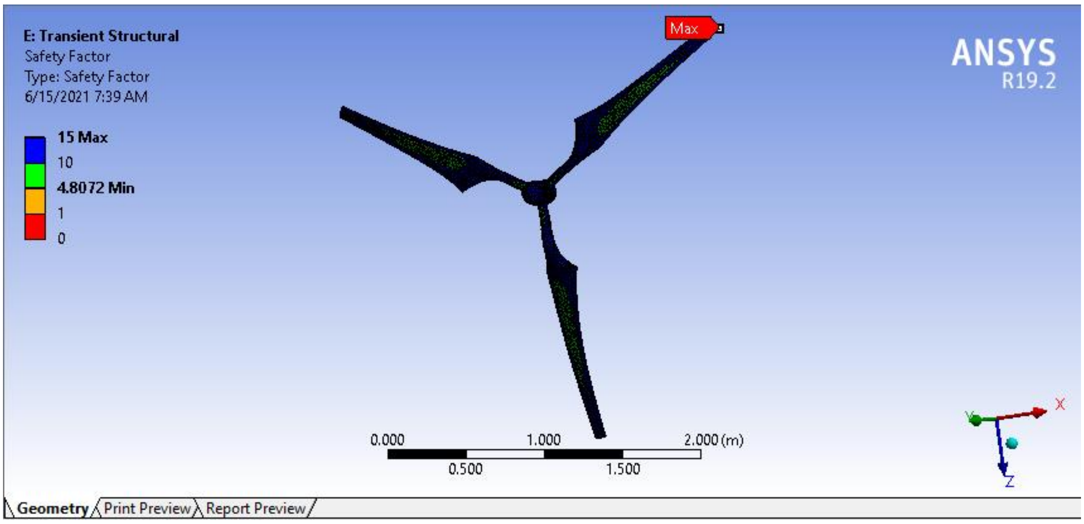

Figure 47: Rotor Structural Analysis (Water) - Factor of Safety

From the figure, the minimum factor of safety obtained for rotor in water configuration was:

$$Minimum\ FoS_{wind} = 4.8072$$

Which means that the rotor is too safe for any type of transient stresses acting on it due to water.

4.2.3 Gear Train Analysis – Wind

The structural analysis for the two-stage transmission system (gear train) for wind configuration was done by analyzing each stage separately. The purpose was just to evaluate the stresses generated at the contact of the gear teeth. The results are discussed below:

4.2.3.1 First Stage – Wind

The Frictional Stresses obtained for the first stage of wind transmission system are shown below:

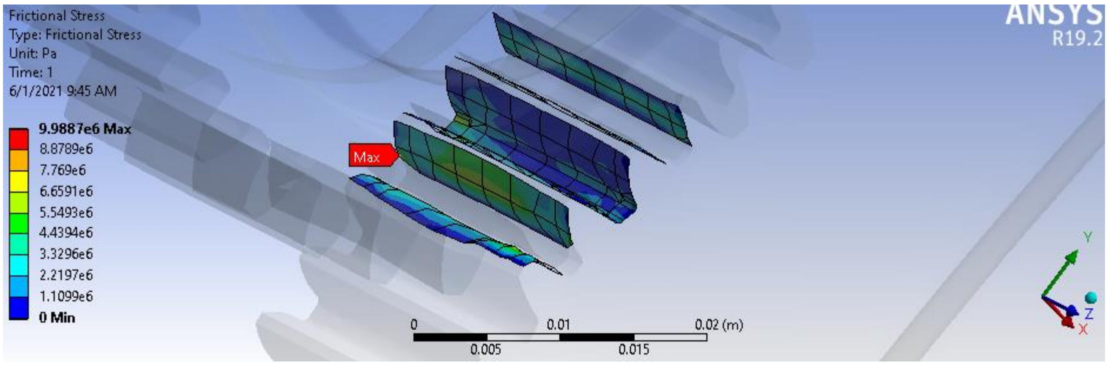

Figure 48: Gear Train Structural Analysis - Wind - Stage 01

From the figure, it can be seen that the maximum frictional stress acting upon the first-stage gears interface is 9.9887 MPa .

4.2.3.2 Second Stage – Wind

The Frictional Stresses obtained for the second stage of wind transmission system are shown below:

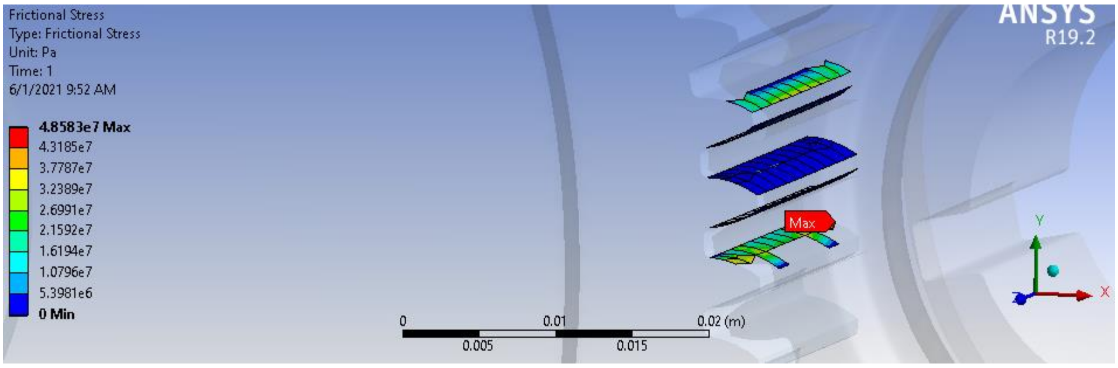

Figure 49: Gear Train Structural Analysis - Wind - Stage 02

From the figure, it can be seen that the maximum frictional stress acting upon the second-stage gears interface is 48.583 MPa .

4.2.4 Gear Train Analysis – Water

Similarly, the structural analysis for the two-stage transmission system (gear train) for water configuration was done by analyzing each stage separately. Just like the case of wind transmission, only the stresses at gear teeth were evaluated. The results are discussed below:

4.2.4.1 First Stage – Water

The Frictional Stresses obtained for the first stage of water transmission system are shown below:

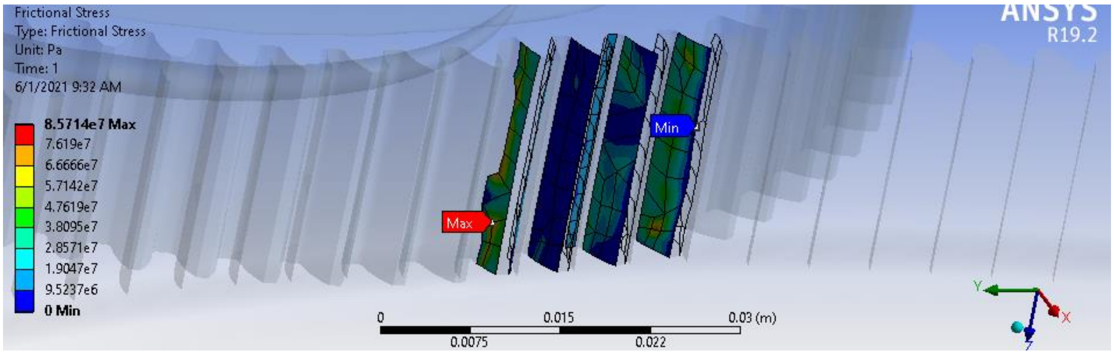

Figure 50: Gear Train Structural Analysis - Water - Stage 01

From the figure, it can be seen that the maximum frictional stress acting upon the first-stage gears interface is 85.714 MPa .

4.2.4.2 Second Stage – Water

The Frictional Stresses obtained for the second stage of water transmission system are shown below:

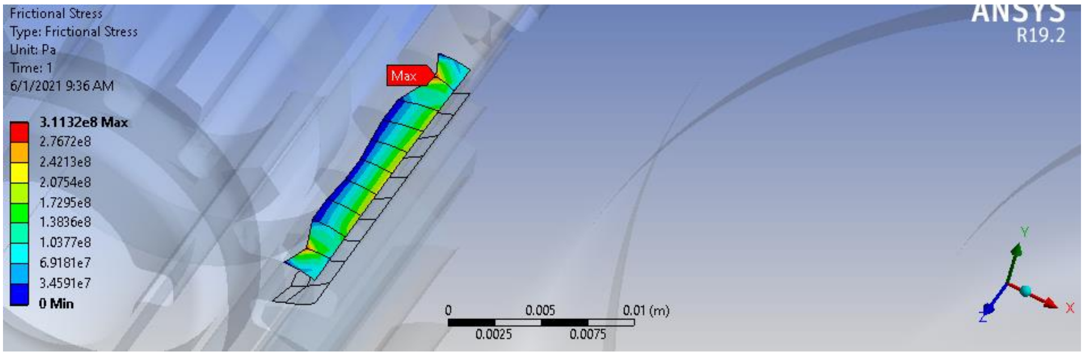

Figure 51: Gear Train Structural Analysis - Water - Stage 02

From the figure, it can be seen that the maximum frictional stress acting upon the second-stage gears interface is 311.32 MPa .

5 CONCLUSIONS & RECOMMENDATIONS

5.1 Conclusions

The above results clearly show that the power production in case of wind is almost half of 1000W. This was already expected because in order to account for size in water configuration the blade radius was reduced, hence decrease in power production. The calculated TSR for wind is in close proximity to the assumed value. The structural analysis shows that for wind configuration the proposed design was safe to a very great extent. Stresses generated were well below the strength of chosen material. The value of strain and deformation were also very small.

For the case of water configuration, the turbine power production was around double of 1000W. The reason being the increase blade length from the calculated one for water configuration only. Again, the achieved TSR value for water configuration was found to be in close proximity of the assumed value. Structural integrity was also not compromised for water configuration as well. The factor of safety achieved proposed that the design is safe to good extent. Value of stresses generated were below the strength of the material and strain and deformation were also reasonably low.

For both configurations it was found that the loads were more in the region of roots of the blade to the middle of the blade. As blade basically behave as a cantilever beam so this region is of interest from failure and breakage point of view.

A lighter material than Aluminum 2018 t61 alloy with less strength can be used as it was found that structural integrity is not compromised for both configurations. Hence, the weight of the turbine can be further reduced without exceeding the limits of structural strength.

It can be inferred that power production capacity is dictated by the operation of the turbine in wind configuration as defines the lower power capacity of the turbine. The structural limits are defined by the operation in water configuration as water imparts higher loads on the turbine, hence, dictating the upper limits of the structural strength of the design.

5.2 Recommendations

A very fine and authentic analysis is always possible when the constraint of good computational power is not present. This constraint forces the use of simplification and assumptions to reduce the complexities of the problem.

The above analysis done, also faced the problem of computational power. Following are some recommendations which enacted upon will increase the accuracy of the results obtained

Mesh Refinement:

Refining the mesh is one of the most basic way of improving the results' accuracy. The domain mesh size can be further reduced to improve accuracy and diminish errors. Similarly, mesh refinement for stationary domain can also be utilized.

Y+ Inclusion:

The wall effects are essential to capture. These are not normally incorporated by the mesh so a very fine layer or layers of mesh have to be generated around the wall to capture its effects. To do so a y+ value of around 1 can be used to determine the first layer thickness and thereupon a growth rate of 1.2 can be used. Around 20 to 30 layers are normally sufficient to capture the wall effects. This method is basically known as inflation.

6DOF with Moment of Inertia Analysis:

In order to greatly simplify the problem a rotating domain was specified and rotational velocity was also assigned. However, a better approach is to assign a moment of inertia value to the turbine by enabling the 6 degrees of freedom (DOF). This will allow the turbine to rotate when the fluid flows across it. This is will be accurately as we will observe the rotation of turbine due to the fluid rather than pre-assigning the rotational velocity.

Domain Sizing:

The domain size of the stationary domain can be enlarged to better develop the flow properties before reaching the turbine. This will ultimately to a more accurate and precise solution.

Enhanced Wall Treatment:

Currently standard wall treatment was used which is not much effective for the capturing the wall effects. The usage of enhanced wall treatment, which increases the ability of k-ε model to account for wall effects, can greatly influence the convergence of the solution and lead to better results.

Two-Way System Coupling:

One way coupling was employed for structural analysis. However, a more effective way is to use two-way system coupling. This simultaneously analyzes the flow effects and stresses on the structure. In this way the deformation is changes in the structure are accounted for as the fluid flow and in return how the changed structure affects the fluid flow as well.

REFERENCES:

1. Barlas T.K.; van Kuik, G.A.M. Review of state of the art in smart rotor control research for wind turbines. *Prog. Aerosp. Sci.* 2010, *46*, 1–27.

2. Barlas, T.; Lackner, M. The Application of Smart Structures for Large Wind Turbine Rotor Blades. In *Proceedings of the Iea Topical Expert Meeting; Delft University of Technology: Delft, The Netherlands, 2006.*

3. Wallace AK and Oliver JA (1998) Variable-speed generation controlled by passive elements. International Conference on Electric Machines. Istanbul, Turkey, 2–5 September.

4. Wright AD and Fingersh LJ (2008) Advanced control design for wind turbines part I: Control design, implementation, and initial tests. Technical Report NREL/TP-500-42437. National Renewable Energy Laboratory (NREL), Golden, Colorado, USA.

5. Anyi, M. and Kirke, B., Evaluation of small axial flow hydrokinetic turbines for remote communities. Energy for Sustainable Development, 14(2), pp. 110 – 116, 2010.

6. Ikeda, T., Tanaka, H., Yoshimura, R., Noda, R., Fujii, T. and Liu, H., 2018. 'A robust biomimetic blade design for micro wind turbines.' *Renewable Energy*, 125, pp.155-165

7. E. Chica, F. Pérez, and A. Rubio-Clemente., 2016. Rotor structural design of a hydrokinetic turbine. International Journal of Applied Engineering Research.

8. Nongdhar Deibanehbok, Goswami Bikramjit., 2018. 'Design of Micro Wind Turbine for Low Wind Speed Areas: A Review', *ADBU Journal of Electrical and Electronics Engineering (AJEEE)*, 2(1)

9. Schubel, P. and Crossley, R., 2012. Wind Turbine Blade Design. *Energies*, 5(9), pp.3425-3449.

10. Kolekar, N. and Banerjee, A., 2013. A coupled hydro-structural design optimization for hydrokinetic turbines. *Journal of Renewable and Sustainable Energy*, 5(5), p.053146.

11. Vermaak, H.J., Kusakana, K. and Koko, S.P., Status of micro-hydrokinetic river technology in rural applications: A review of literature. Renewable and Sustainable Energy Reviews, 29(0), pp. 625–633, 2014.
12. Shinomiya, L., Vaz, J., Mesquita, A., De Oliveira, T., Brasil Jr, A. and Silva, P., 2015. AN APPROACH FOR THE OPTIMUM HYDRODYNAMIC DESIGN OF HYDROKINETIC TURBINE BLADES. *Revista de Engenharia Térmica*, 14(2), p.43.

13. https://ied.eu/blog/sustainable-development-goals-and-the-2030-agenda-how-ied-supports-sdgs/

14. https://www.weforum.org/agenda/2018/05/one-simple-chart-shows-why-an-energy-revolution-is-coming-and-who-is-likely-to-come-out-on-top

15. https://www.irena.org/newsroom/articles/2018/May/New-Estimates-Show-Rapid-Growth-in-Off-Grid-Renewables
16. https://www.weforum.org/reports/accelerating-access-to-sustainable-energy-a-key-priority-in-energy-transition
17. https://www.smart-hydro.de/renewable-energy-systems/hydrokinetic-turbines-river-canal/
18. https://www.weforum.org/agenda/2018/05/one-simple-chart-shows-why-an-energy-revolution-is-coming-and-who-is-likely-to-come-out-on-top
19. https://www.energy.gov/eere/wind/how-do-wind-turbines-work

APPENDIX A: MATLAB Code for NACA Airfoil Generation & Pre-Design Calculations:

```
v_wind= 7;          %wind speed in m/s
v_water=1.6;        %water speed in m/s
TSR_wind= 7;        %Wind tip speed ratio
TSR_water= 5;       %Water tip speed ratio
rho_water= 998;     %water density in kg/m^3
mu_water=1.002e-3; %dynamic viscosity of water
mu_wind=2.857e-5;  %dynamic viscosity of water
rho_wind= 1.0585;  %air density at 1500m altitude in Kg/m^3
P_water= 1000;      %turbine power in W
P_wind= 1000;       %turbine power in W
eta_overall= 0.7;  %conservative value is used accounts for generator,electrical invertor and gearbox
efficiency
Cp_wind= 0.45;      %max value
n=3;                %no.of blades
%theta is pitch angle of turbine

%Calculations for water configuration
%Determination of Cp and r
for i= 1:3
    theta(i)= ((i-1)*5) * pi/180;
    lambda(i) = 1/(1/(TSR_water+0.08*theta(i))-0.035/((theta(i).^3)+1));
    Cp_water(i) = 0.22*(116/lambda(i)-(0.4*theta(i))-5)*exp(-12.5/lambda(i));
end

Cp_water= max(Cp_water(i));
sprintf('Max value of Cp for water is %f',Cp_water)
r_water= ((2*P_water)/(rho_water*pi*Cp_water*eta_overall*(v_water^3)))^0.5;
sprintf('radius for water turbine is %f m',r_water)


%Calculations for wind configuration
r_wind= ((2*P_wind)/(rho_wind*pi*Cp_wind*eta_overall*(v_wind^3)))^0.5;
sprintf('radius for wind turbine is %f m',r_wind)

%Determining radius for hybrid purpose
R_avg= (r_water+r_wind)/2;      %Average blade length
sprintf('The average blade length is %f',R_avg)
R=R_avg;                        %combined blade length
k=10;                           %no of sections, 2 sections for circular profile
r_inc=R/k;                      %relative length increment

%Determining RPMs for both configurations
omega_water=(TSR_water*v_water)/R;          %rotational speed for water
omega_wind=(TSR_wind*v_wind)/R;             %rotational speed for air
N_water=(omega_water*60)/(2*pi);            %RPM for water
N_wind=(omega_wind*60)/(2*pi);              %RPM for air

%Determination of chord length for water configuration
%Determination of axial induction factor "a"
syms a
a= solve(eta_overall*Cp_water==4*a*(1-a)^2,a);
a= double(a);
```

```
a= real(a);
for i=1:3
   if a(i)<=0.5     %momentum theory is valid for this range
      a_imp = a(i);
      a_imp=double(a_imp);
      sprintf('axial induction factor is %f',a_imp)
   end
end


%Calculations for tangential induction factor "a_prime"
syms a_prime
a_prime = solve(a_prime*(1+a_prime)*((TSR_water)^2)==a_imp*(1-a_imp),a_prime);
a_prime=double(a_prime);
a_prime=real(a_prime);
for j=1:2
   if a_prime(j)>0
      a_prime_imp=a_prime(j);
      a_prime_imp=double(a_prime_imp);
      sprintf('the tangential induction factor is %f',a_prime_imp)
   end
end

%Calculations for relative flow angle
phi=atan((1-a_imp)/(TSR_water*(1+a_prime_imp)));
phi=double(phi);
phi=real(phi);
phi_deg=phi*180/pi;
phi_deg=double(phi_deg);
sprintf('angle of relative water flow is %f degrees',phi_deg)

alpha=linspace(0,15,101);
Ma_water=0;          %mach number in water.Speed of sound is normally in range of 1400-1500 m/s so
effectively Ma is almost 0
c_iter_water= 0.027;  %assumed value of chord length
c_water=0;           %initialize value of c--chord length so that value from workspace is not used but
redefined
while abs(c_iter_water-c_water)> 10e-3
   c_water=c_iter_water;
   Re_water= (rho_water*v_water*c_water)/mu_water       %Reynolds number
   sol=xfoil('NACA 24012',alpha,Re_water,Ma_water,'oper iter 150');
   Cl_water=sol.CL;
   Cd_water=sol.CD;
   L_by_D_water=rdivide(Cl_water,Cd_water);        %Calculates lift to drag ratio
   [x,index]=max(L_by_D_water);                    %Gives the index at which max value occurs
   Cd_max_water=Cd_water(index);                   %Gives value of drag coefficient for max Cl/Cd
   Cl_max_water=Cl_water(index);                   %Gives value of lift coefficient for max Cl/Cd


   c_iter_water=(8*a_prime_imp*R_avg*TSR_water*(sin(phi))^2)/(((Cl_max_water*sin(phi))-
(Cd_max_water*cos(phi)))*n*(1-a_imp));     %to calculate chord length
   c_iter_water=double(c_iter_water);
end

c_water=c_iter_water;
sprintf('the chord length for is %f meters when Cl=%f and Cd=%f for Re=%f and
Cl/Cd=%f',c_water,Cl_max_water,Cd_max_water,Re_water,Cl_max_water/Cd_max_water)
alpha_opt_water=sol.alpha(index);       %Gives value of alpha against min Cd
sprintf('the angle of attack is %f degrees for water',alpha_opt_water)
```

```
%Determination of chord length for wind configuration
alpha_wind=linspace(0,15,101);
Ma_wind=0;
c_iter_wind=0.07          %initial assumed value
c_wind=0;                 %To initialize chord length
while abs(c_iter_wind-c_wind)> 10e-3
    c_wind=c_iter_wind;
    Re_wind= (rho_wind*v_wind*c_wind)/mu_wind       %Reynolds number
    sol=xfoil('NACA 24012',alpha_wind,Re_wind,Ma_wind,'oper iter 150');
    Cl_wind=sol.CL;
    Cd_wind=sol.CD;
    L_by_D_wind=rdivide(Cl_wind,Cd_wind);          %Calculates lift to drag ratio
    [x,index]=max(L_by_D_wind);                    %Gives the index at which max value occurs
    Cd_max_wind=Cd_wind(index);                    %Gives value of drag coefficient for max Cl/Cd
    Cl_max_wind=Cl_wind(index);                    %Gives value of lift coefficient for max Cl/Cd
    c_iter_wind= (16*pi*R_avg)/(9*n*Cl_max_wind*TSR_wind*sqrt((TSR_wind)^2+(4/9)))  %to
calculate chord length
    c_iter_wind=double(c_iter_wind);
end

c_wind=c_iter_wind;
sprintf('the chord length for is %f meters when Cl=%f and Cd=%f for Re=%f and
Cl/Cd=%f',c_wind,Cl_max_wind,Cd_max_wind, Re_wind,Cl_max_wind/Cd_max_wind)
alpha_opt_wind=sol.alpha(index);
sprintf('the angle of attack is %f degrees for air',alpha_opt_wind)

%Combined values at each section
c_avg=(c_water+c_wind)/2;                     %combined chord length
Re_avg=(Re_water+Re_wind)/2;                  %combined Reynolds number
TSR_avg=(TSR_water+TSR_wind)/2;                       %combined TSR
sprintf('The combined values at tip are radius= %f,chord= %f,Re= %f and TSR=
%f',R,c_avg,Re_avg,TSR_avg)
VarNames= {'Section', 'Chord Length at section', 'Length at section','Aerodynamic Centre'};
fprintf(1,'%s\t\t%s\t\t%s\t\t%s\n',VarNames{:})
for i=1:(k-2)
    c_section(i)=c_avg*R/(r_inc*(i+2));   %chord length at different sections
    AC_secion(i)=0.25*c_section(i);       %Aerodynamic centre. Generally 25% of chord
    fprintf(1,'%f\t\t\t%f\t\t\t\t%f\t\t\t\t%f\n',i+2,c_section(i),R/k*(i+2),AC_secion(i))
end
```